Nonlinear Dyn (2024) 112:2349–2366
https://doi.org/10.1007/s11071-023-09077-3

ORIGINAL PAPER

Is large-scale vaccination sufficient for controlling the COVID-19 pandemic with uncertainties? A model-based study

Abhijit Majumder · Nandadulal Bairagi

Received: 31 March 2022 / Accepted: 29 October 2023 / Published online: 20 November 2023

Abstract A massive vaccination programme against COVID-19 infection started at the beginning of 2021. Studies show that vaccinated people are subject to reinfection, and there is uncertainty in the rate of immunity loss, the force of infection, recovery rate and vaccine efficacy. Here we study a six-dimensional stochastic epidemic model with vaccine-induced immunity loss to demonstrate the effect of vaccination in controlling the COVID-19 epidemic. It is shown that the disease persists for a long time if the stochastic basic reproduction number $R_{0V}^{S} > 1$ holds. We have also proved a sufficient condition for disease eradication. Our analysis shows that the disease cannot persist if $R_{0V}^{\text{ext}} < 1$. However, this latter condition may not hold if the infectivity increases and/or the vaccine-induced immunity loss increases. Indian and Italian COVID-19 data are used to demonstrate various dynamical behaviours of the system and disease persistence. A non-trivial observation is that mass vaccination cannot eradicate the disease if the vaccine-induced immunity loss is high. Disease eradication is also challenging with the ongoing immunization process if the infectivity of the virus is also high. These results decipher that the infection will last long unless a long-lasting vaccine candidate appears or a low infectious variant replaces the highly contagious COVID-19 variant.

Keywords Vaccination model · White noise · Basic reproduction number · Asymptotic behaviour · Extinction time · Indian and Italian case studies

1 Introduction

Vaccination against COVID-19 infection started in the UK at the end of 2020 [33]. Presently, ten WHO-recommended vaccine candidates are in use throughout the globe [42]. A good proportion of the population is vaccinated in the one year of its application [7]. Though the COVID-19 pandemic has not been controlled, its morbidity and mortality have significantly reduced due to vaccination [35,36]. Numerous mathematical models have been proposed and analysed to determine the course of the COVID-19 pandemic since the WHO announced the public health emergency of international concern (PHEIC) on 30 January 2020 [41] to restrict the spread of the novel coronavirus. These are mainly deterministic SEIR epidemic models or their variants [2,17,25,26,29,30,32,38]. A few are stochastic models [1,16,19,40,45]. Obviously, these earlier models did not consider the effect of vaccination and can no longer be used for the epidemic

A. Majumder · N. Bairagi
Department of Mathematics, Centre for Mathematical Biology and Ecology, Jadavpur University, Raja Subodh Chandra Mallick Road, Kolkata 700032, India
e-mail: nbairagi.math@jadavpuruniversity.in

A. Majumder (✉)
Department of Mathematics, College of Engineering and Technology, SRM Institute of Science and Technology, Chengalpet District, Kattankulathur 603203, Tamilnadu, India
e-mail: abhijitmajumder1991@gmail.com

course once the full-fledged COVID-19 vaccination has started. Any current time epidemic model should contain a vaccinated class. Recently, some researchers have proposed and analysed some COVID-19 vaccination models to find the effect of immunization on the disease dynamics [11,12,18,27,28,34,39,44]. A case study of Japan shows that reduced vaccine efficacy and roll-out of COVID-19 restriction may lead to a surge of COVID-19 cases [11]. Ghostine et al. [12] have proposed an enhanced SEIR model, including a vaccination compartment to mimic the spread of the coronavirus epidemic in Saudi Arabia. It is shown that intensifying the vaccination campaign can significantly decrease the number of confirmed cases and deaths. Kurmi and Chouhan [18] analysed an eight-compartment COVID-19 vaccination model using optimal control theory. They investigated the impact of vaccination on the spread of the disease and demonstrated that a combination of community mitigation strategies and vaccination can effectively minimize this pandemic. The simulations, however, were done with a hypothetical parameter set. A COVID-19 vaccination model was studied in [27] to show that the waning of vaccine-induced immunity significantly impacts the disease dynamics. Rabiu and Iyaniwura [34] developed a COVID-19 model to assess the impact of vaccination and immunity waning on the dynamics of the disease. Without considering a precise vaccination class, De la Sen and Ibeas [39] analysed an SEIR-type epidemic model to observe the combined role of vaccination and antiviral drugs in controlling the COVID-19 pandemic. An SEIR-type epidemic model with time delay and vaccination control was considered by Zhai et al. [44]. They have considered the vaccination strategy based on feedback linearization techniques and showed that the disease would persist in the population if there is no vaccination control. All these models are deterministic types and do not consider any uncertainty in the rate parameters. None of these models studied the effect of vaccine-induced immunity loss on the persistence of the disease. However, understanding the dynamics of a novel virus is insufficient if the inherent noise in the rate parameters is not considered. It is reported that there is uncertainty in the COVID-19 infection rate [24]. Due to spatial heterogeneity and other physical factors, there is a significant variation in the COVID-19 recovery time and rate [8,37]. Most importantly, the efficacy of vaccines produced in the shortest time is primarily unknown. It is also unclear how long these vaccines will provide protection against COVID-19 infection and to what extent. Even after taking a total dose of the vaccine, it is now recommended for a booster dose, implying the vaccine's efficacy loss [6,15]. This indicates the existence of many uncertainties in the COVID-19 disease dynamics, its recovery rate and vaccine efficacy. So the question is: Can the existing vaccination drive eradicate the disease? If it is, what should be the parametric condition, given that there are many uncertainties in COVID-19 disease and vaccine efficacy? We answered these questions by analysing a six-dimensional stochastic epidemic model and demonstrated the effect of vaccination in controlling the COVID-19 epidemic. We considered noise in these rate parameters due to the variability in the infection rate, recovery rate and vaccine efficacy and determined the disease persistence and eradication conditions. Using the Indian and Italian COVID-19 data, we estimated the best-fitted parameters and noise intensities for the considered model. We then observed the variational effects of the force of infection, vaccination and immunity waning rate parameters. Our analysis reveals that the COVID-19 disease will persist over the existing vaccine efficacy and transmissibility for a long time.

The remaining portion of this paper is organized in the following sequence. The stochastic COVID-19 vaccination model is proposed in Sect. 2. Analytical results, including disease extinction conditions and stationary distribution of the solutions, are prescribed in Sect. 3. Section 4 shows parameter estimation and two case studies. A discussion is presented in Sect. 5, and the paper ends with a conclusion in Sect. 6.

2 The model

We propose an extended SEIR stochastic compartmental epidemic model to investigate the COVID-19 disease under vaccination. The total human population, $N(t)$, of a region is divided into six mutually exclusive groups, viz. susceptible, exposed, detected infectives, undetected infectives, recovered and vaccinated, which are denoted by S, E, I, A, R and V, respectively. The susceptible individuals are recruited through birth at a rate Λ. After effective contact with a detected or undetected COVID-19 infected individual, susceptible individuals become infected and join the E class, who carry the virus but are not yet infectious. The transmission

probability of COVID-19 infection from the detected and undetected individuals may differ. Assume that κ is the transmission probability of disease due to the contact between susceptible and undetected infected individuals. The same is $(1-\kappa)$ for the contact between the susceptible and detected individuals. If β is the average per capita daily contact, then the susceptible individual that joins the E class is given by $\beta(\frac{(1-\kappa)SI}{N}+\frac{\kappa SA}{N})$. The susceptible individuals are vaccinated at a rate q and join the V class. Since the vaccination of a susceptible individual does not give 100 % immunity against coronavirus, the vaccinated people may again be infected by the undetected and detected individuals, but possibly at a lower rate. Considering η as the vaccination-induced immunity loss, the portion of the vaccinated individuals who join the exposed class at time t is $\eta(\frac{(1-\kappa)SI}{N}+\frac{\kappa SA}{N})$. Observe that it gives the fraction of vaccinated individuals at time t losses immunity after effective interaction with the detected and undetected infected individuals. We call η the vaccine-induced immunity loss parameter or the vaccine efficacy parameter. If $\eta = 0$, then the vaccine will be 100% effective. An exposed class individual spends on an average $\frac{1}{\omega}$ time in E class and then joins either the undetected class with probability δ or the detected class with probability $(1-\delta)$. An average time of $\frac{1}{\gamma_1}$ and $\frac{1}{\gamma}$ are spent by the undetected and detected individuals, respectively, before moving to the recovered class. Recovered people can also lose immunity and join the susceptible class at a rate of g. Natural death at a rate m is incorporated in every compartment, and an additional disease-related death rate d_i is included in the detected class, I. We do not consider any disease-related death in the A class because critically ill individuals, if any, may be shifted to the I class at a rate ν. Since the coronavirus is a novel virus, there are substantial uncertainties in the rate constants, like infection rate [22], recovery rate [3] in A and I classes, and also in the rate of immunity loss [10]. To incorporate this uncertainty, we consider random perturbations to these parameters as follows: $\mp\beta \to \mp\beta + \sigma_1 \mathrm{d}B_1(t)$, $\eta \to \eta + \sigma_2 \mathrm{d}B_2(t)$, $\gamma_1 \to \gamma_1 + \sigma_3 \mathrm{d}B_3(t)$, $\gamma \to \gamma + \sigma_4 \mathrm{d}B_4(t)$, where $B_i(t)$ are standard mutually independent Brownian motions and $\sigma_i^2, i = 1, 2, 3, 4$, are the intensities of the white noises. Similar parametric perturbation has also been considered in other biological models [4,20,21,43,46]. Encapsulating all these assumptions, the stochastic compartmental model for COVID-19 reads

$$
\begin{aligned}
\mathrm{d}S &= \left[\Lambda - qS - \frac{\beta S}{N}\left((1-\kappa)I + \kappa A\right) - mS + gR\right]\mathrm{d}t \\
&\quad - \frac{\sigma_1 S}{N}\left[(1-\kappa)I + \kappa A\right]\mathrm{d}B_1(t), \\
\mathrm{d}E &= \left[\frac{\beta S}{N}\left((1-\kappa)I + \kappa A\right) + \frac{\eta V}{N}\left((1-\kappa)I + \kappa A\right)\right. \\
&\quad \left. - \omega E - mE\right]\mathrm{d}t + \frac{\left[(1-\kappa)I + \kappa A\right]}{N} \\
&\quad \left(\sigma_1 S \mathrm{d}B_1(t) + \sigma_2 V \mathrm{d}B_2(t)\right), \\
\mathrm{d}A &= \left[\delta\omega E - (\gamma_1 + \nu + m)A\right]\mathrm{d}t - \sigma_3 A \mathrm{d}B_3(t), \\
\mathrm{d}I &= \left[(1-\delta)\omega E - (\gamma + m + d_i)I + \nu A\right]\mathrm{d}t \\
&\quad - \sigma_4 I \mathrm{d}B_4(t), \\
\mathrm{d}R &= \left[\gamma_1 A + \gamma I - gR - mR\right]\mathrm{d}t \\
&\quad + \sigma_3 A \mathrm{d}B_3(t) + \sigma_4 I \mathrm{d}B_4(t), \\
\mathrm{d}V &= \left[qS - \frac{\eta V}{N}\left[(1-\kappa)I + \kappa A\right] - mV\right]\mathrm{d}t \\
&\quad - \frac{\sigma_2 V}{N}\left[(1-\kappa)I + \kappa A\right]\mathrm{d}B_2(t). \qquad (1)
\end{aligned}
$$

In each equation, the expression multiplied with $\mathrm{d}t$ is called the drift coefficient and the expression multiplied with $\mathrm{d}B_i(t)$ is called the diffusion coefficient.

The initial values for the state variables are considered as

$$
S(0) \geq 0,\ E(0) \geq 0,\ A(0) \geq 0,\ I(0) \geq 0,\ R(0) = 0,\ V(0) = 0. \qquad (2)
$$

3 Results

It is to be noted that the system (1) considers the human population as its variables which must be non-negative and bounded. Also, from a dynamical point of view, the solution of the system (1) should exist uniquely. The multiplicative noise considered in (1) may cause a population explosion. It is, therefore, imperative to show that the supposed system has a unique solution without any population explosion, i.e. the solution is global, and all the solutions are positive when starting with positive initial values. We have the following theorem for these results.

Theorem 1 *For any initial value* $(S(0), E(0), A(0), I(0), R(0), V(0)) \in \mathbb{R}^6_+$, *there exists a unique global solution of the system (1) such that* $(S(t), E(t), A(t), I(t), R(t), V(t)) \in \mathbb{R}^6_+$ *for all* $t \geq 0$ *and the solution remains in* $\mathbb{R}^6_+$ *with probability* 1, *i.e. almost surely (a.s).*

Proof See Appendix I for its proof. □

It is worth mentioning that the stochastic system (1) has no equilibrium point. However, it may have some stationary distribution, meaning that no significant change will occur in the asymptotic solution of the system when the time is substantial. From an epidemic point of view, such distribution implies the long-term persistence of the disease. We show that the stationary distribution occurs if the following theorem holds good. We adopted the technique given in [13] to prove this result. The following lemma will be used in the sequel.

Lemma 1 [47] *Let $X(t)$ be a regular Markov process (time-homogeneous) in $\mathbb{R}_+^n$ whose dynamics is described by the stochastic equation*

$$dX(t) = b(X)t + \Sigma_{r=1}^{k} h_r(X)dB_r(t). \tag{3}$$

Then the corresponding diffusion matrix is defined as

$$A(x) = \left[a_{ij}\right], \quad a_{ij} = \Sigma_{r=1}^{k} h_r^i(X)h_r^j(X)$$

and the solution $X(t)$ of (3) has a unique stationary distribution $\pi(.)$ if there exist a bounded domain $U \in R^n$ with regular boundary Γ and (a) there is a positive number M_2 such that $\Sigma_{i,j=1}^{l} a_{ij}(x)\xi_i\xi_j \geq M_2|\xi|^2$, (b) there exist a non-negative C^2-function V_1 such that LV_1 is negative for any $\mathbb{R}_+^n$ for all $x \in \mathbb{R}_+^n$, where $f(.)$ is a function integrable with respect to the measure π.

Theorem 2 *Assume that*

$$R_{0V}^S = \frac{\omega(\beta m + \eta q)}{(q + m + \frac{1}{2}\sigma_1^2)(\gamma + m + d_i + \frac{1}{2}\sigma_4^2)} \times \frac{\{\kappa\delta(\gamma + m + d_i) + (1-\kappa)(\delta\nu + (1-\delta)(\nu + \gamma_1 + m))\}}{(\nu + \gamma_1 + m + \frac{1}{2}\sigma_3^2)(\omega + m + \frac{1}{2}(\sigma_1^2 + \sigma_2^2))}.$$

Then, for any initial value $(S(0), E(0), A(0), I(0), R(0), V(0)) \in \mathbb{R}_+^6$, a sufficient condition for existing a stationary distribution $\pi(.)$ of the system (1) is $R_{0V}^S > 1$.

Proof By Theorem 1, for any initial size of population $(S(0), E(0), A(0), I(0), R(0), V(0)) \in \mathbb{R}_+^6$, there exists a unique non-local global solution $(S, E, A, I, R, V) \in \mathbb{R}_+^6$. Let us denote $D = \frac{1}{N}[(1-\kappa)I + \kappa A]$. The diffusion matrix of the system (1) is given by

$$A' = \begin{pmatrix} \sigma_1^2S^2D^2 & 0 & 0 & 0 & 0 & 0 \\ 0 & \sigma_1^2S^2D^2 + \sigma_2^2V^2D^2 & 0 & 0 & 0 & 0 \\ 0 & 0 & \sigma_3^2A^2 & 0 & 0 & 0 \\ 0 & 0 & 0 & \sigma_4^2I^2 & 0 & 0 \\ 0 & 0 & 0 & 0 & \sigma_3^2A^2 + \sigma_4^2I^2 & 0 \\ 0 & 0 & 0 & 0 & 0 & \sigma_2^2V^2D^2 \end{pmatrix}.$$

Let $\bar{D}_\alpha$ be a bounded domain in $\mathbb{R}_+^6$ which excludes the origin. Choose $M_1 = \min_{(S,E,A,I,R,V)\in\bar{D}_\alpha\in\mathbb{R}_+^6}\{\sigma_1^2S^2D^2, (\sigma_1^2S^2 + \sigma_2^2V^2)D^2, \sigma_3^2A^2, \sigma_4^2I^2, \sigma_3^2A^2 + \sigma_4^2I^2, \sigma_2^2V^2D^2\}$. For $\bar{\zeta} = (\bar{\zeta_1}, \bar{\zeta_2}, \bar{\zeta_3}, \bar{\zeta_4}, \bar{\zeta_5}, \bar{\zeta_6}) \in \mathbb{R}_+^6$, we obtain

$$\begin{aligned} &\Sigma_{i,j=1}^{6} a_{ij}(S, E, A, I, R, V)\bar{\zeta_i}\bar{\zeta_j} = \sigma_1^2S^2D^2\bar{\zeta_1}^2 \\ &+ (\sigma_1^2S^2 + \sigma_2^2V^2)D^2\bar{\zeta_2}^2 + \sigma_3^2A^2\bar{\zeta_3}^2 + \sigma_4^2I^2\bar{\zeta_4}^2 \\ &+ (\sigma_3^2A^2 + \sigma_4^2I^2)\bar{\zeta_5}^2 + \sigma_2^2V^2D^2\bar{\zeta_6}^2, \\ &(S, E, A, I, R, V) \in \bar{D}_\alpha. \end{aligned}$$

Thus, the condition (a) of Lemma 1 holds. In order to prove the second assertion of the lemma, define a non-negative C^2 function H_1, where $H_1 : \mathbb{R}_+^6 \to \mathbb{R}$ be such that $H_1 = (S + E + A + I + R + V) - B_1\ln S - B_2\ln E - B_3\ln A - B_4\ln I$, where B_1, B_2, B_3 and B_4 are positive constants to be determined later.

Applying Ito formula, one gets

$$\begin{aligned} &\mathcal{L}(S + E + A + I + R + V) = \Lambda - m(S + E + A + I + R + V) - d_iI, \\ &\mathcal{L}(-\ln S) = -\frac{\Lambda}{S} + \frac{\beta}{N}[\kappa A + (1-\kappa)I] + q + m - \frac{gR}{N} + \frac{1}{2N^2}\sigma_1^2[\kappa A + (1-\kappa)I]^2, \\ &\mathcal{L}(-\ln E) = -\frac{\eta V}{NE}[\kappa A + (1-\kappa)I] - \frac{\eta V}{NE}[\kappa A + (1-\kappa)I] + \omega + m + \frac{1}{2N^2E^2}(\sigma_1^2S^2 + \sigma_2^2V^2)[\kappa A + (1-\kappa)I]^2, \\ &\mathcal{L}(-\ln A) = -\frac{\delta\omega E}{A} + (\gamma_1 + \nu + m) + \frac{1}{2}\sigma_3^2, \\ &\mathcal{L}(-\ln I) = -\frac{(1-\delta)\omega E}{I} - \frac{\nu A}{I} + (\gamma + m + d_i) + \frac{1}{2}\sigma_4^2. \end{aligned}$$

Therefore, we have

$$\begin{aligned} \mathcal{L}H_1 = {} & \Lambda - m(S + E + A + I + R + V) - d_iI \\ & + B_1\left(-\frac{\Lambda}{S} + \frac{\beta}{N}[\kappa A + (1-\kappa)I] + q + m - \frac{gR}{N} + \frac{1}{2N^2}\sigma_1^2[\kappa A + (1-\kappa)I]^2\right) \\ & + B_2\left(-\frac{\beta S}{NE}[\kappa A + (1-\kappa)I] + \omega + m - \frac{\eta\beta V}{NE}[\kappa A + (1-\kappa)I] + \frac{1}{2N^2E^2}(\sigma_1^2S^2 + \sigma_2^2V^2)[\kappa A + (1-\kappa)I]^2\right) \\ & + B_3\left(-\frac{\delta\omega E}{A} + (\gamma_1 + \nu + m) + \frac{1}{2}\sigma_3^2\right) \end{aligned}$$

$$
\begin{aligned}
&+B_4\left(-\frac{(1-\delta)\omega E}{I}-\frac{\nu A}{I}+(\gamma+m+d_i)+\frac{1}{2}\sigma_4^2\right)\\
&\le -4\left(m(S+E+A+I+R+V)\frac{\Lambda B_1}{S}\frac{\beta S B_2\kappa A}{NE}\right)^{\frac{1}{4}}\\
&\times\left(\frac{\delta\omega B_3 E}{A}\right)^{\frac{1}{4}}\\
&+\left(q+m+\frac{1}{2}\sigma_1^2\right)B_1+\Lambda+\left(\omega+m\right.\\
&\left.+\frac{1}{2}(\sigma_1^2+\sigma_2^2)\right)B_2+\left(\gamma_1+\nu+m+\frac{1}{2}\sigma_3^2\right)B_3\\
&+\left(\gamma+m+d_i+\frac{1}{2}\sigma_4^2\right)B_4-d_iI\\
&+\frac{1}{N}\beta(\kappa A+(1-\kappa)I)B_1\\
&-\frac{\beta(1-\kappa)SI}{NE}B_2-\frac{gR}{N}B_1\\
&-\frac{\beta V}{NE}(\kappa A+(1-\kappa)I)B_2-\frac{(1-\delta)\omega E}{I}B_4\\
&-\frac{\nu A}{I}B_4. \qquad (4)
\end{aligned}
$$

Define $B_1 = \frac{(\beta m+\eta q)(\kappa\delta(\gamma+m+d_i)+(1-\kappa)\delta\nu+(1-\kappa)(1-\delta)(\gamma_1+\nu+m))}{\left(q+m+\frac{1}{2}\sigma_1^2\right)m\beta\kappa\delta\left(\gamma+m+d_i+\frac{1}{2}\sigma_4^2\right)}$ and let

$$
\begin{aligned}
\Lambda &= \left(\omega+m+\frac{1}{2}(\sigma_1^2+\sigma_2^2)\right),\\
B_2 &= \left(\gamma_1+\nu+m+\frac{1}{2}\sigma_3^2\right),\\
B_3 &= \left(\gamma+m+d_i+\frac{1}{2}\sigma_4^2\right)B_4.
\end{aligned}
$$

Therefore,

$$
\begin{aligned}
B_2 &= \frac{\Lambda}{\left(\omega+m+\frac{1}{2}(\sigma_1^2+\sigma_2^2)\right)},\\
B_3 &= \frac{\Lambda}{\left(\gamma_1+\nu+m+\frac{1}{2}\sigma_3^2\right)},\\
B_4 &= \frac{\Lambda}{\left(\gamma+m+d_i+\frac{1}{2}\sigma_4^2\right)}.
\end{aligned}
$$

Define

$$
\begin{aligned}
R_{0V}^S &= \frac{\omega(\beta m+\eta q)}{(q+m+\frac{1}{2}\sigma_1^2)(\gamma+m+d_i+\frac{1}{2}\sigma_4^2)}\\
&\times\frac{\{\kappa\delta(\gamma+m+d_i)+(1-\kappa)(\delta\nu+(1-\delta)(\nu+\gamma_1+m))\}}{(\nu+\gamma_1+m+\frac{1}{2}\sigma_3^2)(\omega+m+\frac{1}{2}(\sigma_1^2+\sigma_2^2))} \qquad (5)
\end{aligned}
$$

so that (4) becomes

$$
\begin{aligned}
\mathcal{L}H_1 &\le -4\Lambda\left[\left(R_{0V}^S\right)^{\frac{1}{4}}-1\right]+\left(q+m+\frac{1}{2}\sigma_1^2\right)B_1-d_iI\\
&+\frac{1}{N}\beta(\kappa A+(1-\kappa)I)B_1-\frac{\beta(1-\kappa)SI}{NE}B_2-\frac{\nu A}{I}B_4\\
&-\frac{\beta V}{NE}(\kappa A+(1-\kappa)I)B_2-\frac{(1-\delta)\omega E}{I}B_4. \qquad (6)
\end{aligned}
$$

We further define

$$
\begin{aligned}
H_2 &= B_5((S+E+A+I+R+V)-B_1\ln S-B_2\ln E\\
&-B_3\ln A-B_4\ln I)-\ln S-\ln R-\ln V+(S+E+A\\
&+I+R+V)=(B_5+1)(S+E+A+I+R+V)\\
&-(1+B_1B_5)\ln S-B_2B_5\ln E-B_3B_5\ln A-\ln R-\ln V. \qquad (7)
\end{aligned}
$$

Let $W_{k_1}=\left(\frac{1}{k_1},k_1\right)\times\left(\frac{1}{k_1},k_1\right)\times\left(\frac{1}{k_1},k_1\right)\times\left(\frac{1}{k_1},k_1\right)\times\left(\frac{1}{k_1},k_1\right)\times\left(\frac{1}{k_1},k_1\right)$. As $k_1\to\infty$, it is evident that

$$
\begin{aligned}
&\liminf_{(S,E,A,I,R,V)\in\mathbb{R}_+^6\setminus W_{k_1}}\\
&\quad H_2(S,E,A,I,R,V)=+\infty. \qquad (8)
\end{aligned}
$$

Now, we intend to prove that $H_2(S,E,A,I,R,V)$ has the unique smallest value

$$H_2(S(0),E(0),A(0),I(0),R(0),V(0)).$$

Taking partial derivatives of the function $H_2(S,E,A,I,R,V)$ with respect to each state variable, we get

$$
\begin{aligned}
\frac{\partial H_2(S,E,A,I,R,V)}{\partial S} &= 1+B_5-\frac{1+B_1B_5}{S},\\
\frac{\partial H_2(S,E,A,I,R,V)}{\partial E} &= 1+B_5-\frac{B_2B_5}{E},\\
\frac{\partial H_2(S,E,A,I,R,V)}{\partial A} &= 1+B_5-\frac{B_3B_5}{A},\\
\frac{\partial H_2(S,E,A,I,R,V)}{\partial I} &= 1+B_5-\frac{B_4B_5}{I},\\
\frac{\partial H_2(S,E,A,I,R,V)}{\partial R} &= 1+B_5-\frac{1}{R},\\
\frac{\partial H_2(S,E,A,I,R,V)}{\partial V} &= 1+B_5-\frac{1}{V}. \qquad (9)
\end{aligned}
$$

Making each of these partial derivatives equal to zero, one gets $S=\frac{1+B_1B_5}{1+B_5}$, $E=\frac{B_2B_5}{1+B_5}$, $A=\frac{B_3B_5}{1+B_5}$, $I=\frac{B_4B_5}{1+B_5}$, $R=\frac{1}{1+B_5}$, $V=\frac{1}{1+B_5}$ as the unique stagnation point of H_2. Furthermore, the Hesse matrix of the function $H_2(S,E,A,I,R,V)$ at the given initial population

density reads

$$M_1 = \begin{pmatrix} \frac{1+B_1B_5}{S^2(0)} & 0 & 0 & 0 & 0 & 0 \\ 0 & \frac{B_2B_5}{E^2(0)} & 0 & 0 & 0 & 0 \\ 0 & 0 & \frac{B_3B_5}{A^2(0)} & 0 & 0 & 0 \\ 0 & 0 & 0 & \frac{B_4B_5}{I^2(0)} & 0 & 0 \\ 0 & 0 & 0 & 0 & \frac{1}{R^2(0)} & 0 \\ 0 & 0 & 0 & 0 & 0 & \frac{1}{V^2(0)} \end{pmatrix}.$$

Clearly, the matrix M_1 is positive definite. Hence, H_2 attains the smallest value at $\left(\frac{1+B_1B_5}{1+B_5}, \frac{B_2B_5}{1+B_5}, \frac{B_3B_5}{1+B_5}, \frac{B_4B_5}{1+B_5}, \frac{1}{1+B_5}, \frac{1}{1+B_5}\right)$. From the continuity of H_2 and using equation (8), the function $H_2(S, E, A, I, R, V)$ has the unique smallest value $H_2(S(0), E(0), A(0), I(0), R(0), V(0))$ inside $\mathbb{R}^6_+$.

We now define a non-negative C^2 function $H : \mathbb{R}^6_+ \to \mathbb{R}_+$ such that $H(S, E, A, I, R, V) = H_2(S, E, A, I, R, V) - H_2(S(0), E(0), A(0), I(0), R(0), V(0))$. Applying Ito formula on H and using the model (1), one obtains

$$\begin{aligned}
\mathcal{L}(H) \le\ & B_5\Big\{-4\Lambda\left[\left(R^S_{0V}\right)^{\frac{1}{4}} - 1\right] + \left(q + m + \frac{1}{2}\sigma_1^2\right)B_1 \\
& - d_i I - \frac{gR}{N}B_1 - \frac{\beta(1-\kappa)SI}{NE}B_2 \\
& + \frac{1}{N}\beta(\kappa A + (1-\kappa)I)B_1 \\
& - \frac{\nu A}{I}B_4 - \frac{\beta V}{NE}(\kappa A + (1-\kappa)I)B_2 - \frac{(1-\delta)\omega E}{I}B_4\Big\} \\
& - \frac{\Lambda}{S} + \frac{\beta}{N}(\kappa A + (1-\kappa)I) + q \\
& + m - \frac{gR}{N} + \frac{1}{2}\sigma_1^2 - \frac{\gamma_1 A}{R} \\
& - \frac{\gamma I}{R} + g \\
& + m + \frac{1}{2}\sigma_3^2\frac{A^2}{R^2} + \frac{1}{2}\sigma_4^2\frac{I^2}{R^2} - \frac{qS}{V} + m + \frac{1}{2}\sigma_2^2 + \Lambda \\
& + \frac{\beta}{V}[\kappa A + (1-\kappa)I] - d_i I \\
& - m(S + E + A + I + R + V).
\end{aligned} \tag{10}$$

Under the assumption $B_6 = 4\Lambda\left[\left(R^S_{0V}\right)^{\frac{1}{4}} - 1\right] > 0$, (10) becomes

$$\begin{aligned}
\mathcal{L}(H) \le\ & -B_5B_6 - (B_5+1)d_iI + B_1B_5\left(q + m + \frac{1}{2}\sigma_1^2\right) \\
& + (1 + B_1B_5)\frac{\beta}{N}(\kappa A + (1-\kappa)I) - (1 + B_1B_5)\frac{gR}{N} \\
& - \frac{\beta(1-\kappa)\mathrm{SI}}{\mathrm{NE}}B_2B_5 - \frac{B_4B_5\nu A}{I} \\
& - \frac{\gamma_1 A}{R} - \frac{\gamma I}{R} - \frac{\Lambda}{S} + g \\
& - \frac{\beta V}{\mathrm{NE}}(\kappa A + (1-\kappa)I)B_2B_5 - \frac{(1-\delta)\omega E}{I}B_4B_5 \\
& - \frac{qS}{V} + q + 3m + \Lambda + \frac{1}{2}\sigma_1^2 + \frac{1}{2}\sigma_2^2 + \frac{1}{2}\sigma_3^2\frac{A^2}{R^2} \\
& + \frac{1}{2}\sigma_4^2\frac{I^2}{R^2} - mN.
\end{aligned} \tag{11}$$

Consider now the following bounded subset $U = \Big\{\delta_1 < S < \frac{1}{\delta_2},\ \delta_1 < E < \frac{1}{\delta_2},\ \delta_1 < A < \frac{1}{\delta_2},\ \delta_1 < I < \frac{1}{\delta_2},\ \delta_1 < R < \frac{1}{\delta_2},\ \delta_1 < V < \frac{1}{\delta_2}\Big\}$, where $\delta_i > 0$, for $i = 1, 2$, are negligibly small constants to be chosen later on. Now, we divide the domain $\mathbb{R}^6_+ \backslash U$ into the following sub-domains:

$$\begin{aligned}
U_1 &= \{(S, E, A, I, R, V) : 0 < S \le \delta_1\}, \\
U_2 &= \{(S, E, A, I, R, V) : 0 < E \le \delta_1, S > \delta_2\}, \\
U_3 &= \{(S, E, A, I, R, V) : 0 < A \le \delta_1, E > \delta_2\}, \\
U_4 &= \{(S, E, A, I, R, V) : 0 < I \le \delta_1, A > \delta_2\}, \\
U_5 &= \{(S, E, A, I, R, V) : 0 < R \le \delta_2, I > \delta_1\}, \\
U_6 &= \{(S, E, A, I, R, V) : 0 < V \le \delta_1, R > \delta_2\}, \\
U_7 &= \left\{(S, E, A, I, R, V) : S \ge \frac{1}{\delta_2}\right\}, \\
U_8 &= \left\{(S, E, A, I, R, V) : E \ge \frac{1}{\delta_2}\right\}, \\
U_9 &= \left\{(S, E, A, I, R, V) : A \ge \frac{1}{\delta_2}\right\}, \\
U_{10} &= \left\{(S, E, A, I, R, V) : I \ge \frac{1}{\delta_2}\right\}, \\
U_{11} &= \left\{(S, E, A, I, R, V) : R \ge \frac{1}{\delta_2}\right\}, \\
U_{12} &= \left\{(S, E, A, I, R, V) : V \ge \frac{1}{\delta_2}\right\}.
\end{aligned} \tag{12}$$

We have to prove that $\mathcal{L}H(S, E, A, I, R, V) < 0$ on $\mathbb{R}^6_+ \backslash U$, or equivalently, $\mathcal{L}H < 0$ in all of the above twelve regions. We provide proofs of the first two cases. The other cases can be proved with a similar argument.

Case 1. Suppose $(S, E, A, I, R, V) \in U_1$, then (11) becomes

$$\begin{aligned}
\mathcal{L}(H) \le\ & -B_5B_6 - (B_5+1)d_iI \\
& + B_1B_5\left(q + m + \frac{1}{2}\sigma_1^2\right) \\
& + (1 + B_1B_5)\frac{\beta}{N}(\kappa A + (1-\kappa)I) \\
& - (1 + B_1B_5)\frac{gR}{N}
\end{aligned}$$

$$
\begin{aligned}
&-\frac{\beta(1-\kappa)SI}{NE}B_2B_5-\frac{B_4B_5\nu A}{I}-\frac{\Lambda}{\delta_1}\\
&-\frac{\gamma_1 A}{R}-\frac{\gamma I}{R}+g\\
&-\frac{\beta V}{NE}(\kappa A+(1-\kappa)I)B_2B_5\\
&-\frac{(1-\delta)\omega E}{I}B_4B_5-\frac{qS}{V}\\
&+q+3m+\Lambda+\frac{1}{2}\sigma_1^2+\frac{1}{2}\sigma_2^2\\
&+\frac{1}{2}\sigma_3^2\frac{A^2}{R^2}+\frac{1}{2}\sigma_4^2\frac{I^2}{R^2}-mN.
\end{aligned}
$$

Choosing $\delta_1 > 0$ sufficiently small, one obtains $\mathcal{L}(H) < 0$ for every $(S, E, A, I, R, V) \in U_1$.

Case 2. If $(S, E, A, I, R, V) \in U_2$, then from (11), we obtain

$$
\begin{aligned}
\mathcal{L}(H) \le\ & -B_5B_6-(B_5+1)d_iI\\
&+B_1B_5\left(q+m+\frac{1}{2}\sigma_1^2\right)\\
&+(1+B_1B_5)\frac{\beta}{N}(\kappa A+(1-\kappa)I)-(1+B_1B_5)\frac{gR}{N}\\
&-\frac{\beta(1-\kappa)SI}{NE}B_2B_5-\frac{B_4B_5\nu A}{I}\\
&-\frac{\Lambda}{S}-\frac{\gamma_1 A}{R}-\frac{\gamma I}{R}+g\\
&-\frac{\beta V}{NE}(\kappa A+(1-\kappa)I)B_2B_5\\
&-\frac{(1-\delta)\omega E}{I}B_4B_5-\frac{qS}{V}\\
&+q+3m+\Lambda+\frac{1}{2}\sigma_1^2+\frac{1}{2}\sigma_2^2+\frac{1}{2}\sigma_3^2\frac{A^2}{R^2}\\
&+\frac{1}{2}\sigma_4^2\frac{I^2}{R^2}-\frac{m\delta_2}{\delta_1}.
\end{aligned}
$$

Letting $\delta_2^2 = \delta_1$ and choosing large positive value of B_5 and sufficiently small value of δ_2, one have $\mathcal{L}(H) < 0$ for every $(S, E, A, I, R, V) \in U_2$. Similarly, by selecting sufficiently small values of either $\delta_1 > 0$ or $\delta_2 > 0$, it can be easily shown that $\mathcal{L}(H) < 0$ for the rest cases. Thus, $\mathcal{L}(H) < 0$ can be attained for every $(S, E, A, I, R, V) \in U_{12}$. Therefore, condition (b) of Lemma 1 is satisfied, and hence, Theorem 2 is proved, following Lemma 1. □

Remark 1 Here, R_{0V}^S defined in (5) may be called as the stochastic basic reproduction number (SBRN), which ensures the disease establishment in the stochastic system (1) when $R_{0V}^S > 1$.

Remark 2 One can easily obtain (see Appendix II) the deterministic basic reproduction number (DBRN) as $R_{0V}^D = \frac{\omega(\beta m+\eta q)\{\kappa\delta(\gamma+m+d_i)+(1-\kappa)\delta\nu+(1-\kappa)(1-\delta)(\nu+\gamma_1+m)\}}{(q+m)(\gamma+m+d_i)(\nu+\gamma_1+m)(\omega+m)}$.

If $R_{0V}^D > 1$, then disease can be established in the corresponding deterministic system. Observe that the basic reproduction number of the stochastic system (R_{0V}^S) is smaller than that of the corresponding deterministic system (R_{0V}^D). Furthermore, if $\sigma_i = 0, i = 1, .., 4$, then R_{0V}^S coincides with R_{0V}^D.

Observe that both the infected classes (symptomatic and asymptomatic) originate from the exposed class. Thus, the infection will eventually be eradicated if the individuals of the exposed class go extinct. For the system (1), the exposed class $E(t)$ is said to be extinct (i.e. the system will be disease-free) if $\lim_{t\to\infty} E(t) = 0\ a.s.$ [19]. We give here some sufficient conditions for which the exposed class dies out over time. In proving the extinction criterion, the result of the strong law of large number given in the following lemma will be used.

Lemma 2 [31] *Let $M = \{M\}_{t\ge 0}$ be a continuous valued local martingale and vanishing at $t = 0$, then*

$$
lim_{t\to\infty} < M, M_t >< \infty \implies \lim_{t\to\infty}\frac{M_t}{< M, M >_t} = 0,
$$

and

$$
\limsup_{t\to\infty}\frac{< M, M >_t}{t} < 0 \implies \lim_{t\to\infty}\frac{M_t}{t} = 0\ \ a.s.
$$

Theorem 3 *The exposed individuals of the system (1) tend to zero exponentially almost surely if $R_{0V}^{ext} < 1$, where $R_{0V}^{ext} = \frac{1}{\omega+m}\left(\frac{\beta^2}{2\sigma_1^2}+\frac{\eta^2}{2\sigma_2^2}\right)$.*

Proof Assume that $(S(t), E(t), A(t), I(t), R(t), V(t)) \in \mathbb{R}_+^6$ is a solution of system (1) satisfying the initial value $(S(0), E(0), A(0), I(0), R(0), V(0)) \in \mathbb{R}_+^6$. Following Ito's formula, we have

$$
\begin{aligned}
d(\ln E(t)) =\ & \left(\frac{\beta S(\tau)((1-\kappa)I(\tau)+\kappa A(\tau))}{N(\tau)E(\tau)}\right.\\
&\left.-\frac{\sigma_1^2S^2(\tau)((1-\kappa)I(\tau)+\kappa A(\tau))^2}{2N^2(\tau)E^2(\tau)}\right)dt\\
&+\left(\frac{\eta V(\tau)((1-\kappa)I(\tau)+\kappa A(\tau))}{N(\tau)E(\tau)}\right.\\
&\left.-\frac{\sigma_2^2V^2(\tau)((1-\kappa)I(\tau)+\kappa A(\tau))^2}{2N^2(\tau)E^2(\tau)}\right)dt-(\omega+m)\\
&+\frac{\sigma_1 S}{NE}((1-\kappa)I+\kappa A)\,dB_1(t)\\
&+\frac{\sigma_2 V}{NE}((1-\kappa)I+\kappa A)\,dB_2(t).
\end{aligned}
\tag{13}
$$

Upon integration from 0 to t, we have

$$\begin{aligned}\ln E(t) = &\int_0^t \left(\frac{\beta S(\tau)((1-\kappa)I(\tau)+\kappa A(\tau))}{N(\tau)E(\tau)}\right.\\ &\left.-\frac{\sigma_1^2 S^2(\tau)((1-\kappa)I(\tau)+\kappa A(\tau))^2}{2N(\tau)^2E^2(\tau)}\right)dt\\ &+\int_0^t \left(\frac{\eta V(\tau)((1-\kappa)I(\tau)+\kappa A(\tau))}{N(\tau)E(\tau)}\right.\\ &\left.-\frac{\sigma_2^2 V^2(\tau)((1-\kappa)I(\tau)+\kappa A(\tau))^2}{2N^2(\tau)E^2(\tau)}\right)dt\\ &-(\omega+m)\,t+M_1(t)+M_2(t)+\ln E(0),\end{aligned} \tag{14}$$

where $M_1(t)=\int_0^t \frac{\sigma_1 S}{NE}((1-\kappa)I+\kappa A)\,dB_1(\tau)$, $M_2(t)=\int_0^t \frac{\sigma_2 V}{NE}((1-\kappa)I+\kappa A)\,dB_2(\tau)$ are the local continuous martingale with $M_1(0)=0$, $M_2(0)=0$. We, then have $<M_1,M_1>_t=\int_0^t \frac{\sigma_1^2 S^2}{N^2E^2}((1-\kappa)I+\kappa A)^2\,dt<\sigma_1^2$ and $<M_2,M_2>_t=\int_0^t \frac{\sigma_2^2 V^2}{N^2E^2}((1-\kappa)I+\kappa A)^2\,dt<\sigma_2^2$. Using the fact $\max\left(\frac{\beta S(\tau)((1-\kappa)I(\tau)+\kappa A(\tau))}{N}(\tau)E(\tau)-\frac{\sigma_1^2 S^2(\tau)((1-\kappa)I(\tau)+\kappa A(\tau))^2}{2N(\tau)^2E^2(\tau)}\right)=\frac{\beta^2}{2\sigma_1^2}$ and $\left(\frac{\eta V(\tau)((1-\kappa)I(\tau)+\kappa A(\tau))}{N(\tau)E(\tau)}-\frac{\sigma_2^2 V^2(\tau)((1-\kappa)I(\tau)+\kappa A(\tau))^2}{2N^2(\tau)E^2(\tau)}\right)=\frac{\eta^2}{2\sigma_2^2}$, (14) can be written as

$$\begin{aligned}\ln E(t) \le &\left(\frac{\beta^2}{2\sigma_1^2}+\frac{\eta^2}{2\sigma_2^2}-(\omega+m)\right)t\\ &+M_1(t)+M_2(t)+\ln E(0).\end{aligned} \tag{15}$$

Taking the limit superior as $t\to\infty$, after dividing both sides of (15) by t (>0) and using Lemma 2, we have

$$\limsup_{t\to\infty}\frac{\ln E(t)}{t}\le\left(\frac{\beta^2}{2\sigma_1^2}+\frac{\eta^2}{2\sigma_2^2}-(\omega+m)\right)<0. \tag{16}$$

If $\frac{1}{\omega+m}\left(\frac{\beta^2}{2\sigma_1^2}+\frac{\eta^2}{2\sigma_2^2}\right)<1$, then $\lim_{t\to\infty}E(t)=0$ almost surely. Hence, the theorem is proved. □

It is observable that R_{0V}^{ext} is an increasing function of β and η. Thus, if the infection rate increases or the vaccine-induced immunity loss increases, the inequality $R_{0V}^{ext}<1$ may not be held, and consequently, the disease eradication may not be possible.

4 Case study

For the case study, we considered the COVID-19 data from two countries, India and Italy. The parameters estimation and other detailed analysis were done using the Indian COVID-19 epidemic data available from the repositories Covid19India.Org (https://covid19india.org) and Worldometers.info (https://www.worldometers.info/coronavirus/country/india/). The daily and cumulative numbers of infected, recovered, deceased, and vaccinated cases are reported and updated daily in these depositories. The results of Italy were obtained following a similar analysis.

The per day birth rate of new susceptibles is assumed to be constant during the study period. So, we considered this rate Λ as a constant. However, the parameters, infection spreading rate β, probability of joining from the exposed class to the undetected class δ, the recovery rates γ_1, γ, the death rate d_i, vaccination-induced immunity loss rate η and vaccination rate (q) are all subject to be different at different time. For example, β is different because the severity of the contagious nature of the COVID-19 virus is different due to the different infectivity of the virus strain. The parameter value of δ may be different because of the different policies imposed by the government from time to time. The parameters γ_1, γ, d_i, η are also different as the different COVID-19 strains have different fatalities, and different individuals have different immunity levels, and the presence of comorbidities and other immunosuppression factors. The vaccination rate (q) is also not uniform throughout the period as it depends on the vaccine availability and the infrastructure level. It is unexpected to have a single data set for the long vaccination period of any country that will best fit the actual data. Instead, it will be more worthwhile to adopt the method of piecewise fitting the actual data with the vaccine model (1).

We have considered India's COVID-19 data for 2 February 2021 to 7 July 2022. Different variants of Covid-19 have different infectivity and virulence. Furthermore, the vaccination rate was low initially but increased subsequently. We, therefore, divided the data set of the study period into five intervals to obtain a good fit parameter set: (1) from 2 February 2021 to 6 May 2021 (the date when the peak is attained in the second wave); (2) from 7 May 2021 to 27 December 2021 (end of the second wave); (3) from 28 December 2021 to 20 January 2022 (the date when the peak of the third wave is attained); (4) from 21 January 2022 to 15 April 2022 (end of the third wave); and (5) from 16 April 2022 to 7 July 2022, where study period ends. We fitted (see Fig. 1) the actual COVID-19 data (in red colour) for the considered period with the stochastic model solution (in blue colour). Table 1 provides the best-fitted parameters and optimal noise intensities. The Italian COVID-19 data (available from the repository ourworldindata.org

Table 1 Estimated parameter values of system (1) for Indian COVID-19 data for the periods: (1) 2 February 2021 to 6 May 2021; (2) 7 May 2021 to 27 December 2021; (3) 28 December 2021 to 20 January 2022; (4) from 21 January 2022 to 15 April 2022; (5) from 16 April 2022 to 7 July 2022

Period	Λ	m	β	κ	δ	ω	γ	γ_1	g	d_i	ν	η	q	σ_1	σ_2	σ_3	σ_4
1	77756	4.1×10^{-5}	0.115	0.92	0.66	0.18	0.03	0.032	0.004	0.007	0.002	0.11	1.6×10^{-3}	0.03	0.02	.035	0.04
2	77756	4.1×10^{-5}	0.109	0.92	0.66	0.18	0.014	0.16	0.064	0.018	0.002	0.23	2.1×10^{-3}	0.06	0.05	0.04	0.05
3	77756	4.1×10^{-5}	0.57	0.92	0.97	0.18	0.004	0.205	0.14	0.017	0.002	0.23	4×10^{-3}	0.09	0.08	0.12	0.1
4	77756	4.1×10^{-5}	0.090	0.92	0.99	0.18	0.004	0.364	0.42	0.024	0.002	0.12	4.8×10^{-3}	0.14	0.11	0.07	0.4
5	77756	4.1×10^{-5}	0.134	0.92	0.66	0.18	0.029	0.030	0.0004	0.013	0.002	0.15	2.5×10^{-3}	0.015	0.023	0.031	0.03

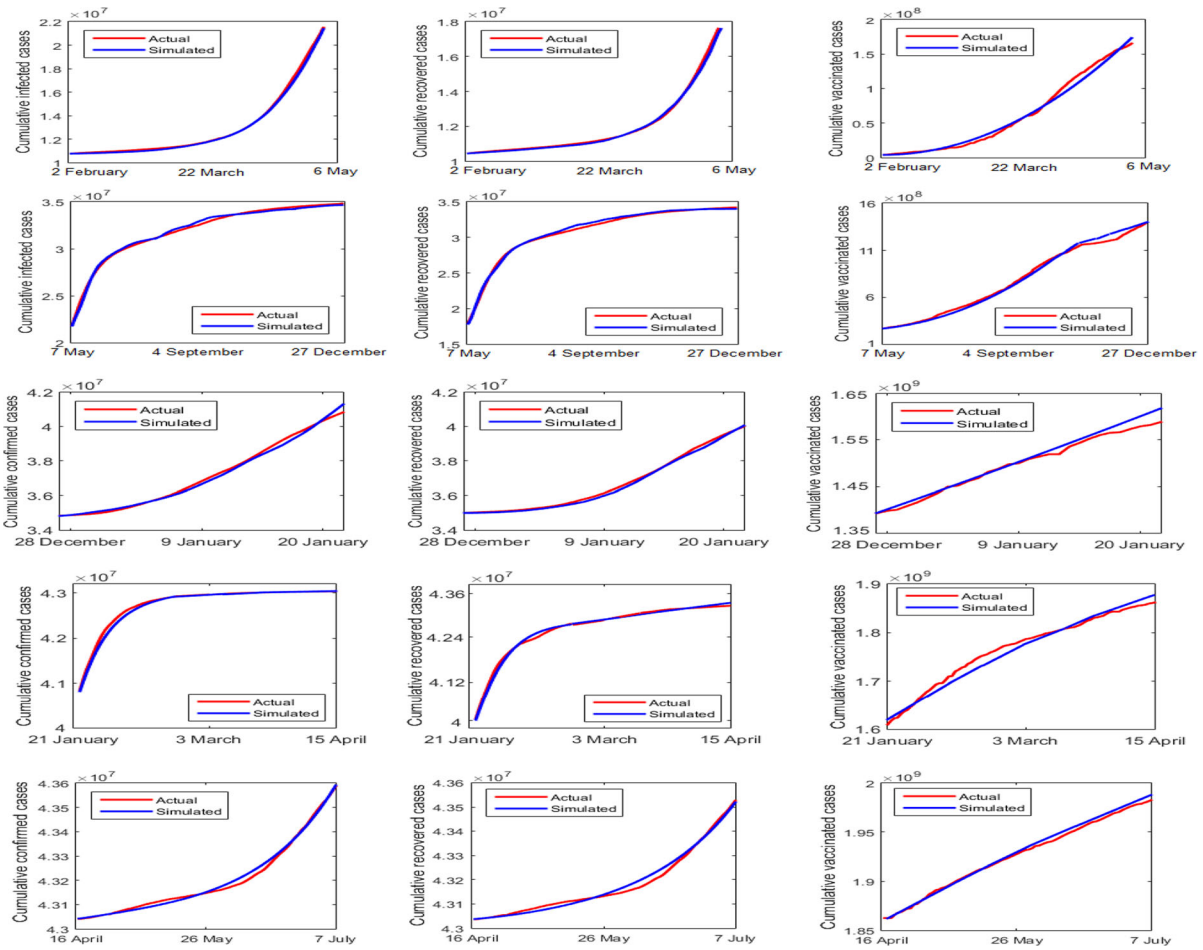

Fig. 1 COVID-19 data fitting with the parameter values and noise intensities as in Table 1. The first row provides the cumulative actual COVID-19 data (red-coloured curve) of the confirmed, recovered and vaccinated cases in India from 2 February 2021 to 5 May 2021. The solution (blue-coloured curve) of the stochastic model (1) is the fitted curve with the parameter values of the first row of Table 1. The other rows represent the same consecutive periods mentioned in Table 1

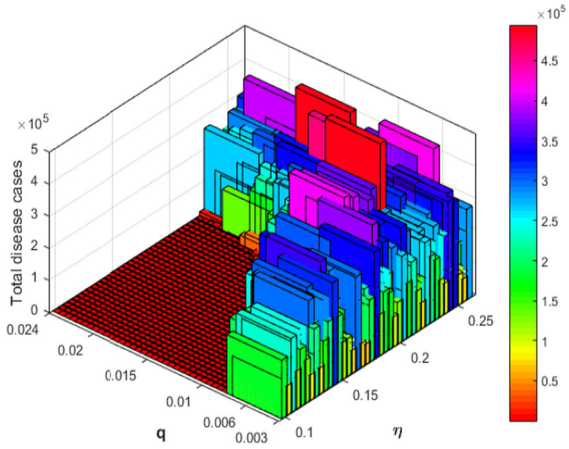

Fig. 2 Per day COVID-19 positive cases in India for the variation in the rate parameters η and q, representing the immunity loss and vaccination rate, respectively. The total disease cases (asymptotic plus symptomatic) are the end values of the solutions for 1000 time steps. Noise intensities and other parameter values remain fixed from 28 December 2021 to 20 January 2022 (see Table 1, third row), the increasing phase of COVID-19 cases of the last wave

(https://ourworldindata.\\org/covid-cases), used for the study period 11 October 2021 to 7 July 2022, were divided into three time segments: (1) from 11 October 2021 to 18 January 2022 (the date when the peak is attained in the second wave); (2) from 18 January 2022 to 20 April 2022 (peak is attained in third wave); (3) from 21 April 2022 to 7 July 2022 (where the study period ends). As in the case of Indian COVID-19 data fitting, we fitted (see Fig. 7) the actual COVID-19 data (red colour) of Italy with the model generated data (blue colour). The best-fitted parameters and the optimal noise intensities are provided in Table 2. The parameters and noise estimation techniques are given in Appendix III.

Indian COVID-19 vaccination programme started on 16 January 2021 [5]. Though the initial vaccination rate was slow, it intensified later on. We demonstrated how the vaccination rate (q) and the immunity loss rate (η) jointly influence the disease burden. We also explained why the COVID-19 positive cases increased during the third wave even after mass vaccination. To elucidate, we considered the parameter values of the third row (see Table 1), representing the increasing phase of the third wave, and plotted (Fig. 2) the per day COVID-19 positive cases ($A+I$) from the solution of system (1) for simultaneous variation in q and η. The parameters q and η were varied in the range $0-0.024$ and $0.1-0.25$, respectively. The lower range value of each parameter was considered smaller than all the estimated values of the said parameter (see

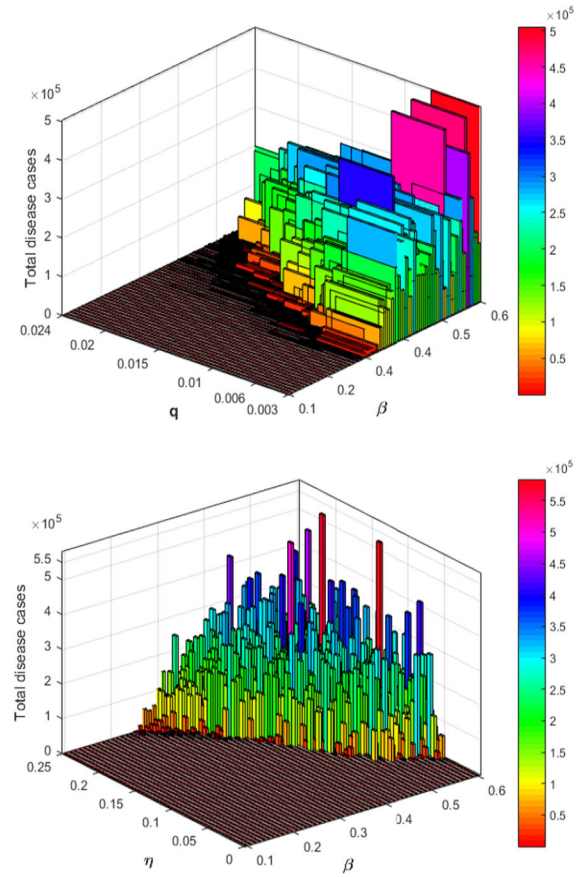

Fig. 3 Per day COVID-19 positive cases with respect to β and q (up) and β and η (down). Noise intensities and other parameter values remain fixed for the period of 28 December 2021 to 20 January 2022, see Table 1

Table 1), and the value at the higher range was considered larger than all the estimated values. It shows that daily COVID-19 positive cases increase with the increasing vaccination rate (q) when the vaccine-induced immunity loss (η) exceeds the value 0.23, i.e. if the vaccine efficacy is lower than 77%. On the contrary, if vaccine efficacy is higher than 77% (or $\eta < 0.23$), then daily COVID-19 positive cases decrease with increasing immunization. Observe that the per day cases become as high as 0.397 million when $\eta = 0.25$ and $q = 0.22$. It is to be mentioned that Indian COVID-19 positive cases during the peak (20^{th} January) of the third wave were reported as 0.34 million per day (https://www.worldometers.info/coronavirus/country/india/). Thus, increased vaccination cannot eradicate COVID-19 infection if the vaccine efficacy is low; instead, it increases the COVID-19 cases. However, infection eradication is possible with a higher vaccination rate if the vaccine immunity is more than

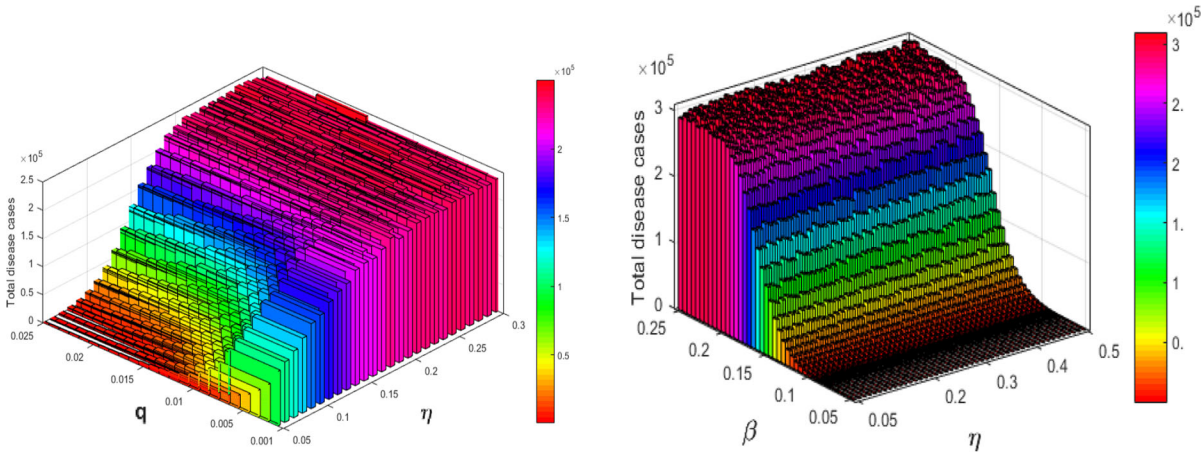

Fig. 4 Left: Per day COVID-19 positive cases in Italy for the variation in the rate parameters η and q, representing the immunity loss and vaccination rate, respectively. The total disease cases (asymptotic plus symptomatic) are the end values of the solutions for 1000 time steps. Right: same for the variation of β and η. Noise intensities and other parameter values remain fixed in the period from 21^{st} April 2022 to 7^{th} July 2022 (see Table 2)

77%. It is to be mentioned that $R_{0V}^S < 1$ holds for the lower values of q and η; $R_{0V}^S > 1$ for its higher values.

A similar phenomenon is plotted in Fig. 3 (up) when the vaccination rate (q) and force of infection (β) are varied simultaneously. The COVID-19 positive cases gradually increase if β is high and q is low. The number of positive cases may be as high as 0.5 million per day at the low vaccination and high transmission rates (below figure). In the opposite case, the disease is eradicated. The lower figure represents the newly infected per day COVID-19 cases when the force of infection (β) and the vaccine efficacy (η) parameters are jointly varied. The infection spreads rapidly when $\beta > 0.25$ and $\eta > 0.2$ (Fig. 3, below). The COVID-19 cases in this parametric range may be as high as 0.532 million per day. It is also to be noted that the number of COVID-19 cases will be few if β is high and η is low. It demonstrates that vaccine effectiveness is crucial in controlling the COVID-19 cases. The disease may be controlled even at a very high infection rate if the vaccine efficacy is close to 100% (i.e. η is close to zero). On the other hand, daily COVID-19 cases will remain under control if β is low and η is significantly high. Thus, a strain of coronavirus with low infectivity would not sustain at the present immunization rate.

We plotted a similar figure as in the case study for India (Fig. 2) to explore how the number of disease cases in Italy would change under the variation of parameters q and η. In the case of Italy, we observe (Fig. 4, left) that if the vaccination-induced immunity loss is higher

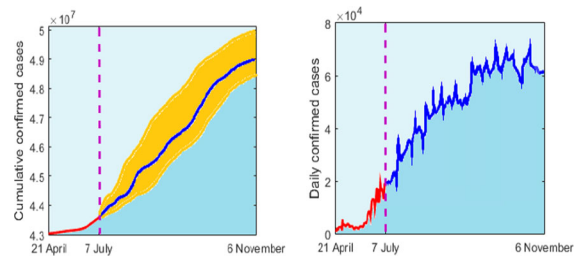

Fig. 5 Left: Predicted cumulative COVID-19 confirmed cases in India for the next 150 days starting 7 July 2022. The simulation results of the system (1) (blue line) predict that India may observe 4.88×10^7 positive cases until the first week of November 2022. The confidence interval (95%) is plotted with a yellow shed. Right: Predicted daily confirmed cases for the same period. The red curve in both figures indicates the actual cases, and the dotted vertical line indicates 7 July 2022. Parameters and noise intensities as in the last row of Table 1

than 12%, the epidemic will rapidly grow. In case of variation of β and η, it is observed that when β is low (< 0.1), number of confirmed cases is low (Fig. 4, right). However, confirmed cases increase rapidly for a higher transmission rate.

Indian COVID-19 cases are again in increasing mode. We predicted the cumulative confirmed COVID-19 positive cases for the next 150 days based on the current epidemiological status of India. To provide a forecast, we repeated the stochastic system's solution 1000 times and then took the mean to get the estimated values with a 95 % confidence interval (blue line of Fig. 5, left). The

Table 2 Estimated parameter values of system (21) for Italian COVID-19 data for the periods: (1) 11 October 2021 to 18 January 2022; (2) 19 January 2022 to 20 April 2022; and (3) 21 April 2022 to 7 July 2022

Period	Λ	m	β	κ	δ	ω	γ	γ_1	g	d_i	ν	η	q	σ_1	σ_2	σ_3	σ_4
1	1428	3.35×10^{-5}	0.228	0.88	0.66	0.16	0.025	0.035	0.035	0.003	0.004	0.32	4.2×10^{-4}	0.12	0.50	.23	0.21
2	1428	3.35×10^{-5}	0.118	0.88	0.66	0.16	0.025	0.035	0.065	0.003	0.004	0.45	1×10^{-4}	0.11	0.10	0.08	0.10
3	1428	3.35×10^{-5}	0.208	0.88	0.66	0.16	0.025	0.038	0.065	0.0026	0.004	0.45	5×10^{-5}	0.10	0.07	0.18	0.16

See Appendix IV for curve fitting

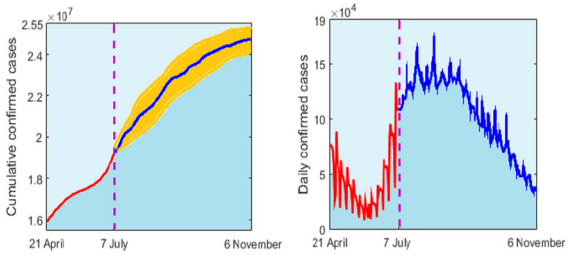

Fig. 6 Left: Predicted cumulative COVID-19 confirmed cases in Italy for the next 150 days starting 7 July 2022. The simulation results of the system (1) (blue line) predict that Italy may observe 2.49×10^7 positive cases until the first week of November 2022. The confidence interval (95%) is plotted with a yellow shed. Right: Predicted daily confirmed cases for the same period. The red curve in both figures indicates the actual cases; the dotted vertical line means 7 July 2022. Parameters and noise intensities as in the last row of Table 2

curve is increasing and will continue till the first week of November 2022, indicating that the newly infected cases are surging gradually. The cumulative number of the predicted infected case till the first week of November 2022 might be between 4.82×10^7 to 5.01×10^7 in the 95% confidence interval. The predicted daily COVID-19 confirmed cases in India till the first week of November 2022 are presented in Fig. 5, right. The COVID-19 cases in Italy also exhibit an increasing trend. Figure 6 indicates that the daily case may be around 37,142 and the cumulative cases might be between 2.41×10^7 to 2.54×10^7 till the first week of November 2022. It is, however, to be mentioned that the accurate prediction for a significantly long period is quite impossible in the case of COVID-19 infection because this novel virus can mutate to some strains with high infectivity [14]. Also, a change in the control measure imposed by the authority can change the trend.

5 Discussion

The COVID-19 infection has put the world under pressure for more than two years. Most countries have experienced several waves of this infection at the cost of millions of lives. A massive vaccination programme started at the end of 2020, hoping the disease would be controlled. Though the morbidity and mortality of the COVID-19 disease reduced significantly, disease eradication, even of its control, is far from expected. In the second and third waves, many countries experienced higher positive cases than the previous peak values. Several European countries, the UK and the USA have fully vaccinated a significant proportion of their population but cannot resist further COVID-19 infection. This fact has put the efficacy of the vaccine under question. Recent studies show that vaccine-induced immunity is significantly reduced after six to eight months post-vaccination. The level of a COVID-19 antibody that persists after this period may not be sufficient to prevent reinfection. There is, however, uncertainty regarding the immunity loss rate among the vaccinated population. Uncertainty also exists in different rate parameters, e.g. the force of infection and recovery rates. It is undoubtedly true that the infectivity of the omicron variant is much higher than the previous strains. Also, the severity of the disease is relatively low, and the recovery rate is high in the current wave caused due to the omicron variant of coronavirus. Thus, there are many uncertainties in the COVID-19 disease dynamics, the force of infection, recovery rate, vaccine availability and administration. The efficacy of vaccines and their protection duration is unclear even after receiving the full vaccine dose. There is also uncertainty regarding the immunity loss rate among the vaccinated population. Therefore, we searched for the answer to whether existing vaccination drives eradicate the disease. What would be the parametric condition for disease eradication through vaccination in the presence of various uncertainties?

Considering such uncertainties in the rate parameters, we have proposed and analysed a six-dimensional stochastic COVID-19 epidemic model in the presence of vaccination to know whether the ongoing vaccination drive can eliminate the disease. We used the theories of the asymptotic behaviour of the nonlinear stochastic sys-

tem to analyse this noise-induced dynamical system. We here prescribed both the disease persistence and eradication conditions. It is shown that the disease indeed persists for a long time if the stochastic basic reproduction number (SBRN) is greater than unity. It is noticed that this value of SBRN is smaller than the DBRN (deterministic basic reproduction number) of the corresponding deterministic model, which is usually considered a measure of disease establishment in the latter type of epidemic models. A sufficient condition ($R_{0V}^{\text{ext}} < 1$) is established for the disease eradication from the system. Noticeably, this condition may not hold if the disease's infectivity increases and/or the vaccine-induced immunity loss increases (i.e. if the vaccine efficacy is reduced). Both issues are probably real for many countries, where vaccination starts in the initial months of 2021, implying that vaccinated people will significantly lose their immunity from July/August onwards (seven to eight months post-vaccination). Furthermore, the new variant, omicron, is highly infectious. These two reasons are probably responsible for the second, third and subsequent waves in different countries. We used the Indian and Italian COVID-19 data to demonstrate the variational effects of the rate parameters q, η and β. Noticeably, if the vaccine-induced immunity loss rate, η, is higher than 0.23 for India, eradicating infection is practically impossible. The same value of η for Italy is 0.12. The COVID-19 positive cases will surge in India if the force of infection is high (> 0.25) and vaccine-induced immunity loss is higher than 20%. For Italy, these values are 0.1 and 12%, respectively. It implies that the disease will last long unless a long-lasting vaccine candidate appears or a low infectious variant replaces the highly contagious variant.

There are, however, some limitations of this model. For example, this model does not consider the population's age structure. It is to be mentioned that a higher age group population is more prone to COVID-19 infection. Secondly, there are many variants of coronavirus with different infectivity and virulence. Therefore, a multi-strain epidemic model would be more appropriate to represent the ongoing pandemic. Despite such limitations, our theoretical and simulation results justify the reason for long-lasting disease persistence even when a large-scale immunization process has been implemented. To our knowledge, such effects have not been reported earlier using a dynamic mathematical model.

6 Conclusion

Nonlinear analysis of a six-dimensional stochastic epidemic model reveals that eradicating COVID-19 infection is challenging if the vaccine-induced immunity loss or the infectivity of the virus strain is high. Therefore, the disease will last long unless a long-lasting vaccine candidate appears or a low infectious variant replaces the highly contagious variant. Using the method described here, one can estimate the required vaccination rate when the vaccine-induced immunity loss or the infectivity of the disease is known, and vice versa. The authority may use it in the immunization and disease eradication process of COVID-19.

Acknowledgements Research of Abhijit Majumder is supported by CSIR (File No: 09/096(0874)/2017-EMR-I). Research of N.B. is supported by SERB, India, Ref. No.: MSC/2020/000020.

Data availability The data sets that support the results of this study are taken from the Worldometer website (https://www.worldometers.info/coronavirus/country/india/) and from the Ourworldindata website (https://ourworldindata.org/covid-cases) which are freely available repositories.

Declarations

Conflict of interest The authors declare that they have no conflict of interest.

Appendices

Appendix 1

Since the coefficients of the model system (1) are locally Lipschitz continuous, for any $\Big(S(0), E(0), A(0), I(0), R(0), V(0)\Big) \in \mathbb{R}^6_+$, there is a unique local solution $\Big(S(t), E(t), A(t), I(t), R(t), V(t)\Big) \in \mathbb{R}^6_+$ for all $t \in [0, \tau_e)$, where τ_e is the explosion time [23]. We now prove $\tau_e = \infty$ a.s. so that the solution becomes global. Let $\kappa_0 > 0$ be sufficiently large for every coordinate $\Big(S(0), E(0), A(0), I(0), R(0), V(0)\Big)$ lying within the interval $\left[\frac{1}{\kappa_0}, \kappa_0\right]$. We then define, for every integer $\kappa > \kappa_0$, the stopping time

$$\tau_\kappa = \inf\left\{t \in [0, \tau_e) : S(t) \notin \left(\frac{1}{\kappa}, \kappa\right),\ E(t) \notin \left(\frac{1}{\kappa}, \kappa\right),\ A(t) \notin \left(\frac{1}{\kappa}, \kappa\right),\ I(t) \notin \left(\frac{1}{\kappa}, \kappa\right),\ R(t) \notin \left(\frac{1}{\kappa}, \kappa\right),\ V(t) \notin \left(\frac{1}{\kappa}, \kappa\right)\right\}. \tag{17}$$

Thus, τ_κ is increasing as $\kappa \to \infty$. Set $\lim_{\kappa\to\infty} \tau_\kappa = \tau_\infty$, when $\tau_\infty \leq \tau_e$ a.s. We now show that $\tau_\infty = \infty$ by a contradiction. Let us assume that our claim is not true and there exist two constants $T_2 > 0$ and $\epsilon \in (0, 1)$ such that $P(\tau_\infty \leq T_2) > \epsilon$. Thus, there exists an integer $\kappa_1 \geq \kappa_0$ such that

$$P(\tau_\kappa \leq T_2) \geq \epsilon, \quad \forall\, \kappa \geq \kappa_1. \tag{18}$$

Noticing that $u + 1 - \ln u > 0$ for all $u > 0$ and $(S(t), E(t), A(t), I(t), R(t), V(t)) \in \mathbb{R}^6_+$, we define the following positive definite function

$$L = (S + 1 - \ln S) + (E + 1 - \ln E) + (A + 1 - \ln A) + (I + 1 - \ln I) + (R + 1 - \ln R) + (V + 1 - \ln V).$$

Applying Ito's formula, one can have

$$\begin{aligned}
\mathrm{d}L &= \left(1 - \frac{1}{S}\right)\mathrm{d}S + \frac{1}{2S^2}(\mathrm{d}S)^2 + \left(1 - \frac{1}{E}\right)\mathrm{d}E \\
&\quad + \frac{1}{2E^2}(\mathrm{d}E)^2 + \left(1 - \frac{1}{A}\right)\mathrm{d}A + \frac{1}{2A^2}(\mathrm{d}A)^2 \\
&\quad + \left(1 - \frac{1}{I}\right)\mathrm{d}I + \frac{1}{2I^2}(\mathrm{d}I)^2 + \left(1 - \frac{1}{R}\right)\mathrm{d}R \\
&\quad + \frac{1}{2R^2}(\mathrm{d}R)^2 + \left(1 - \frac{1}{V}\right)\mathrm{d}V + \frac{1}{2V^2}(\mathrm{d}V)^2 \\
&= \left(1 - \frac{1}{S}\right)\left[\left(\Lambda - qS - \frac{\beta S}{N}((1-\kappa)I + \kappa A) - mS \right.\right. \\
&\quad \left.\left. + gR\right)\mathrm{d}t - \frac{\sigma_1 S}{N}((1-\kappa)I + \kappa A)\,\mathrm{d}B_1(t)\right] \\
&\quad + \frac{1}{2N^2}\sigma_1^2((1-\kappa)I + \kappa A)^2\mathrm{d}t \\
&\quad + \left(1 - \frac{1}{E}\right)\left[\left(\frac{\beta S}{N}((1-\kappa)I + \kappa A)\right.\right. \\
&\quad \left.\left. + \frac{\eta V}{N}((1-\kappa)I + \kappa A) - (\omega + m)E\right)\mathrm{d}t \right. \\
&\quad \left. + \frac{[(1-\kappa)I + \kappa A]}{N}(\sigma_1 S\mathrm{d}B_1(t) + \sigma_2 V\mathrm{d}B_2(t))\right] \\
&\quad + \frac{1}{2N^2E^2}(\sigma_1^2 S^2 + \sigma_2^2 V^2)((1-\kappa)I + \kappa A)^2\mathrm{d}t \\
&\quad + \left(1 - \frac{1}{A}\right)\left[\left(\delta\omega E - (\gamma_1 + \nu + m)A\right)\mathrm{d}t \right. \\
&\quad \left. - \sigma_3 A\mathrm{d}B_3(t)\right] + \frac{1}{2}\sigma_3^2\mathrm{d}t + \left(1 - \frac{1}{I}\right)\left[\left((1-\delta)\omega E \right.\right. \\
&\quad \left.\left. - (\gamma + m + d_i)I + \nu A\right)\mathrm{d}t - \sigma_4 I\mathrm{d}B_4(t)\right] + \frac{1}{2}\sigma_4^2\mathrm{d}t \\
&\quad + \left(1 - \frac{1}{R}\right)\left[(\gamma_1 A + \gamma I - gR - mR)\,\mathrm{d}t + \sigma_3 A\mathrm{d}B_3(t) \right. \\
&\quad \left. + \sigma_4 I\mathrm{d}B_4(t)\right] + \frac{1}{2R^2}(\sigma_3 A\mathrm{d}B_3(t) + \sigma_4 I\mathrm{d}B_4(t))^2 \\
&\quad + \left(1 - \frac{1}{V}\right)\left[\left(qS - \frac{\eta V}{N}[(1-\kappa)I + \kappa A] - mV\right)\mathrm{d}t \right. \\
&\quad \left. - \frac{\sigma_2 V}{N}[(1-\kappa)I + \kappa A]\,\mathrm{d}B_2(t)\right] \\
&\quad + \frac{\sigma_2^2}{2N^2}[(1-\kappa)I + \kappa A]^2\mathrm{d}t.
\end{aligned}$$

Noting $u \leq 2(u + 1 - \ln u)$ for all $u > 0$ and N is the total population, the above expression becomes

$$\begin{aligned}
\mathrm{d}L &\leq \left[\Lambda + 6m + q + \beta + \nu + d_i + g + \omega + \gamma_1 + \gamma + d_i \right. \\
&\quad \left. + \eta + \frac{1}{2}(\sigma_3^2 + \sigma_4^2)\left(1 + \left(\frac{\Lambda}{m}\right)^2\right) + 2(S + 1 - \ln S) \right. \\
&\quad \left. + 2\omega(E + 1 - \ln E) + 2\gamma_1(A + 1 - \ln A) + \sigma_1^2 + \sigma_2^2 \right. \\
&\quad \left. + 2\gamma(I + 1 - \ln I)\right]dt + 2(R + 1 - \ln R) \\
&\quad + 2(V + 1 - \ln V) + \frac{\sigma_1}{N}\left\{1 - \frac{S}{E}\right\}[\kappa A \\
&\quad + (1-\kappa)I]\mathrm{d}B_1(t) + \frac{\sigma_2}{N}\left\{1 - \frac{V}{E}\right\}[\kappa A \\
&\quad + (1-\kappa)I]\mathrm{d}B_2(t) + \sigma_3\left\{1 - \frac{A}{R}\right\}\mathrm{d}B_3(t) \\
&\quad + \sigma_4\left\{1 - \frac{I}{R}\right\}\mathrm{d}B_4(t).
\end{aligned}$$

Let $\Delta_1 = \Lambda + 6m + q + \beta + \nu + d_i + g + \omega + \gamma_1 + \gamma + d_i + \eta + \frac{1}{2}(\sigma_3^2 + \sigma_4^2)\left(1 + \left(\frac{\Lambda}{m}\right)^2\right) + \sigma_1^2 + \sigma_2^2$ and $\Delta_2 = \max\{1, \omega, \gamma, \gamma_1\}$. Then

$$\begin{aligned}
dL &\leq (\Delta_1 + \Delta_2 L)\mathrm{d}t + \frac{\sigma_1}{N}\left\{1 - \frac{S}{E}\right\} \\
&\quad [\kappa A + (1-\kappa)I]\mathrm{d}B_1(t) \\
&\quad + \frac{\sigma_2}{N}\left\{1 - \frac{V}{E}\right\}[\kappa A + (1-\kappa)I]\mathrm{d}B_2(t) \\
&\quad + \sigma_3\left\{1 - \frac{A}{R}\right\}\mathrm{d}B_3(t) + \sigma_4\left\{1 - \frac{I}{R}\right\}\mathrm{d}B_4(t).
\end{aligned}$$

Defining $\Delta_3 = \max\{\Delta_1, \Delta_2\}$, we have

$$\begin{aligned}
\mathrm{d}L &\leq \Delta_3(1 + L)\mathrm{d}t + \frac{\sigma_1}{N}\left\{1 - \frac{S}{E}\right\} \\
&\quad [\kappa A + (1-\kappa)I]\mathrm{d}B_1(t) \\
&\quad + \frac{\sigma_2}{N}\left\{1 - \frac{V}{E}\right\}[\kappa A + (1-\kappa)I]\mathrm{d}B_2(t) \\
&\quad + \sigma_3\left\{1 - \frac{A}{R}\right\}\mathrm{d}B_3(t) + \sigma_4\left\{1 - \frac{I}{R}\right\}\mathrm{d}B_4(t).
\end{aligned} \tag{19}$$

Noticing that

$$\frac{\sigma_1}{N}\left\{1-\frac{S}{E}\right\}[\kappa A+(1-\kappa)I]\le\sigma_1\left(1-\frac{m}{\Lambda}\right),$$
$$\frac{\sigma_2}{N}\left\{1-\frac{V}{E}\right\}[\kappa A+(1-\kappa)I]\le\sigma_2\left(1-\frac{m}{\Lambda}\right),$$
$$\sigma_3\left\{1-\frac{A}{R}\right\}\le\sigma_3\left(1-\frac{m}{\Lambda}\right),$$
$$\sigma_4\left\{1-\frac{I}{R}\right\}\le\sigma_4\left(1-\frac{m}{\Lambda}\right),$$

we have

$$\mathbb{E}\int_0^{\tau_{\kappa_1}\wedge T_2}\left|\frac{\sigma_1}{N}\left\{1-\frac{S}{E}\right\}[\kappa A+(1-\kappa)I]\right|^2\mathrm{d}t<\infty,$$
$$\mathbb{E}\int_0^{\tau_{\kappa_1}\wedge T_2}\left|\frac{\sigma_2}{N}\left\{1-\frac{V}{E}\right\}[\kappa A+(1-\kappa)I]\right|^2\mathrm{d}t<\infty,$$
$$\mathbb{E}\int_0^{\tau_{\kappa_1}\wedge T_2}\left|\sigma_3\left\{1-\frac{A}{R}\right\}\right|^2\mathrm{d}t<\infty,$$
$$\mathbb{E}\int_0^{\tau_{\kappa_1}\wedge T_2}\left|\sigma_4\left\{1-\frac{I}{R}\right\}\right|^2\mathrm{d}t<\infty.$$

Since all the functions $\frac{\sigma_1}{N}\left\{1-\frac{S}{E}\right\}[\kappa A+(1-\kappa)I]$, $\frac{\sigma_2}{N}\left\{1-\frac{V}{E}\right\}[\kappa A+(1-\kappa)I]$, $\sigma_3\left\{1-\frac{A}{R}\right\}$, $\sigma_4\left\{1-\frac{I}{R}\right\}$ are continuous, bounded and non-anticipative, then for a sequence of partition of the interval $[0,\tau_{\kappa_1}\wedge T_2]$ with mesh size $\Delta t\to 0$, one have

$$\begin{aligned}&\mathbb{E}\int_0^{\tau_{\kappa_1}\wedge T_2}\frac{\sigma_1}{N}\left\{1-\frac{S}{E}\right\}[\kappa A+(1-\kappa)I]\mathrm{d}B_1(t)\\&=\lim_{\Delta t\to 0}\Sigma_j\mathbb{E}\frac{\sigma_1}{N(t_j)}\left\{1-\frac{S(t_j)}{E(t_j)}\right\}\\&\quad[\kappa A(t_j)+(1-\kappa)I(t_j)]\\&\quad\times\mathbb{E}(B_1(t_{j+1})-B_1(t_j))\\&\left[\because\ \frac{\sigma_1}{N(t_j)}\left\{1-\frac{S(t_j)}{E(t_j)}\right\}[\kappa A(t_j)+(1-\kappa)I(t_j)]\text{ and }\right.\\&\left.B_1(t_{j+1})-B_1(t_j)\text{ are independent}\right].\end{aligned}$$

Similarly, we have

$$\begin{aligned}&\mathbb{E}\int_0^{\tau_{\kappa_1}\wedge T_2}\frac{\sigma_2}{N}\left\{1-\frac{V}{E}\right\}[\kappa A+(1-\kappa)I]\mathrm{d}B_2(t)\\&=\lim_{\Delta t\to 0}\Sigma_j\mathbb{E}\frac{\sigma_2}{N(t_j)}\left\{1-\frac{V(t_j)}{E(t_j)}\right\}\\&\quad[\kappa A(t_j)+(1-\kappa)I(t_j)]\\&\quad\times\mathbb{E}(B_2(t_{j+1})-B_2(t_j)),\\&\mathbb{E}\int_0^{\tau_{\kappa_1}\wedge T_2}\sigma_3\left(1-\frac{A}{R}\right)\mathrm{d}B_3(t)\\&=\lim_{\Delta t\to 0}\Sigma_j\mathbb{E}\left(\sigma_3\left(1-\frac{A(t_j)}{R(t_j)}\right)\right)\mathbb{E}(B_3(t_{j+1})-B_3(t_j)),\end{aligned}$$

and

$$\begin{aligned}&\mathbb{E}\int_0^{\tau_{\kappa_1}\wedge T_2}\sigma_4\left(1-\frac{I}{R}\right)\mathrm{d}B_4(t)\\&=\lim_{\Delta t\to 0}\Sigma_j\mathbb{E}\left(\sigma_4\left(1-\frac{I(t_j)}{R(t_j)}\right)\right)\mathbb{E}(B_4(t_{j+1})-B_4(t_j)).\end{aligned}$$

Using the fact that the increment of the Brownian motion is normally distributed with mean zero and variance $(t_{j+1}-t_j)$, we have

$$\mathbb{E}\int_0^{\tau_{\kappa_1}\wedge T_2}\frac{\sigma_1}{N}\left\{1-\frac{S}{E}\right\}[\kappa A+(1-\kappa)I]\mathrm{d}B_1(t)=0,$$
$$\mathbb{E}\int_0^{\tau_{\kappa_1}\wedge T_2}\frac{\sigma_2}{N}\left\{1-\frac{V}{E}\right\}[\kappa A+(1-\kappa)I]\mathrm{d}B_2(t)=0,$$
$$\mathbb{E}\int_0^{\tau_{\kappa_1}\wedge T_2}\sigma_3\left(1-\frac{A}{R}\right)\mathrm{d}B_3(t)=0,$$
$$\mathbb{E}\int_0^{\tau_{\kappa_1}\wedge T_2}\sigma_4\left(1-\frac{I}{R}\right)\mathrm{d}B_4(t)=0.$$

Integrating both sides of (19) from 0 to $\tau_{\kappa_1}\wedge T_2$, taking the expectation and using the above fact, we obtain

$$\begin{aligned}&\mathbb{E}L\Big(S(\tau_{\kappa_1}\wedge T_2),E(\tau_{\kappa_1}\wedge T_2),A(\tau_{\kappa_1}\wedge T_2),I(\tau_{\kappa_1}\wedge T_2),\\&\quad R(\tau_{\kappa_1}\wedge T_2),V(\tau_{\kappa_1}\wedge T_2)\Big)\\&\le L\Big(S(0),E(0),A(0),I(0),R(0),V(0)\Big)\\&\quad+\Delta_3\,\mathbb{E}\int_0^{\tau_{\kappa_1}\wedge T_2}(1+L)\mathrm{d}t\\&\le L\Big(S(0),E(0),A(0),I(0),R(0),V(0)\Big)+\Delta_3T_2\\&\quad+\Delta_3\,E\int_0^{\tau_\kappa\wedge T_2}L\mathrm{d}t.\end{aligned}$$

Since L is an increasing function on $[0,\tau_{\kappa_1}\wedge T_2]$, for any $t\in[0,\tau_{\kappa_1}\wedge T_2]$, $L\Big(S(t),E(t),A(t),I(t),R(t),V(t)\Big)$
$\le L\Big(S(\tau_{\kappa_1}\wedge T_2),E(\tau_{\kappa_1}\wedge T_2),A(\tau_{\kappa_1}\wedge T_2),I(\tau_{\kappa_1}\wedge T_2),$
$R(\tau_{\kappa_1}\wedge T_2),V(\tau_{\kappa_1}\wedge T_2)\Big)$.

$$\begin{aligned}&\therefore\mathbb{E}L\Big(S(\tau_{\kappa_1}\wedge T_2),E(\tau_{\kappa_1}\wedge T_2),A(\tau_{\kappa_1}\wedge T_2),I(\tau_{\kappa_1}\wedge T_2),\\&\quad R(\tau_{\kappa_1}\wedge T_2),V(\tau_{\kappa_1}\wedge T_2)\Big)\\&\le L\Big(S(0),E(0),A(0),I(0),R(0),V(0)\Big)+\Delta_3T_2+\Delta_3\\&\quad\times\mathbb{E}\int_0^{\tau_{\kappa_1}\wedge T_2}L\Big(S(\tau_{\kappa_1}\wedge T_2),E(\tau_{\kappa_1}\wedge T_2),A(\tau_{\kappa_1}\wedge T_2),\\&\quad I(\tau_{\kappa_1}\wedge T_2),R(\tau_{\kappa_1}\wedge T_2),V(\tau_{\kappa_1}\wedge T_2)\Big)\mathrm{d}t\end{aligned}$$

$$\leq L\Big(S(0), E(0), A(0), I(0), R(0), V(0)\Big) + \Delta_3 T_2 + \Delta_3 \times \int_0^{\tau_{\kappa_1}\wedge T_2} \mathbb{E}L\Big(S(\tau_{\kappa_1}\wedge T_2), E(\tau_{\kappa_1}\wedge T_2), A(\tau_{\kappa_1}\wedge T_2), I(\tau_{\kappa_1}\wedge T_2), R(\tau_{\kappa_1}\wedge T_2), V(\tau_{\kappa_1}\wedge T_2)\Big)\,\mathrm{d}t.$$

Gronwall's inequality then gives

$$\begin{aligned}&\mathbb{E}L(S(\tau_{\kappa_1}\wedge T_2), E(\tau_{\kappa_1}\wedge T_2), A(\tau_{\kappa_1}\wedge T_2), I(\tau_{\kappa_1}\wedge T_2), R(\tau_{\kappa_1}\wedge T_2), V(\tau_{\kappa_1}\wedge T_2))\\ &\leq (L(S(0), E(0), A(0), I(0), R(0), V(0)) + \Delta_3 T_2)e^{\Delta_3(\tau_{\kappa_1}\wedge T_2)} = \Delta_4 \text{ (say)}.\end{aligned} \tag{20}$$

Set $\Omega_{\kappa_1} = \{\tau_{\kappa_1} \leq T_2\}$ for all $\kappa_1 \geq \kappa_2$. Thus, following (18), we get $P(\Omega_{\kappa_1}) \geq \epsilon_3$ for all $\omega_2 \in \Omega_{\kappa_1}$. Clearly, at least one of $S(\tau_{\kappa_1}, \omega_2)$, $E(\tau_{\kappa_1}, \omega_2)$, $A(\tau_{\kappa_1}, \omega_2)$ $I(\tau_{\kappa_1}, \omega_2)$, $R(\tau_{\kappa_1}, \omega_2)$, $V(\tau_{\kappa_1}, \omega_2)$ is equal to either κ_1 or $\frac{1}{\kappa_1}$. Hence, $L(S(\tau_{\kappa_1}), E(\tau_{\kappa_1}), A(\tau_{\kappa_1}), I(\tau_{\kappa_1}), R(\tau\kappa_1), V(\tau\kappa_1))$ is no less than $\min\{\kappa_1 + 1 - \ln\kappa_1, \frac{1}{\kappa_1} + 1 + \ln\kappa_1\}$. From (18) and (20), we then obtain

$$\begin{aligned}\Delta_4 &\geq \mathbb{E}[1_{\Omega_{\kappa_1}} L(S(\tau_{\kappa_1}, \omega_2), E(\tau_{\kappa_1}, \omega_2), A(\tau_{\kappa_1}, \omega_2), I(\tau_{\kappa_1}, \omega_2), R(\tau_{\kappa_1}, \omega_2), V(\tau_{\kappa_1}, \omega_2))]\\ &\geq \epsilon_3\left[(\kappa_1 + 1 - \ln\kappa_1) \wedge \left(\frac{1}{\kappa_1} + 1 + \ln\kappa_1\right)\right],\end{aligned}$$

where $1_{\Omega_{\kappa_1}}$ is the indicator function of Ω_{κ_1}. Letting $\kappa_1 \to \infty$, we get $\infty > \Delta_4 = \infty$, a contradiction. Hence, $\tau_\infty = \infty$ a.s. Hence, the theorem is proved.

Appendix 2

One can easily write the deterministic version of the stochastic model (1) as

$$\begin{aligned}\frac{\mathrm{d}S}{\mathrm{d}t} &= \Lambda - qS - \frac{\beta S}{N}[(1-\kappa)I + \kappa A] - mS + gR,\\ \frac{\mathrm{d}E}{\mathrm{d}t} &= \frac{\beta S}{N}[(1-\kappa)I + \kappa A] + \frac{\eta V}{N}[(1-\kappa)I + \kappa A] - \omega E - mE,\\ \frac{\mathrm{d}A}{\mathrm{d}t} &= \delta\omega E - (\gamma_1 + \nu + m)A,\\ \frac{\mathrm{d}I}{\mathrm{d}t} &= (1-\delta)\omega E + \nu A - (\gamma + m + d_i)I,\\ \frac{\mathrm{d}R}{\mathrm{d}t} &= \gamma_1 A + \gamma I - gR - mR,\\ \frac{\mathrm{d}V}{\mathrm{d}t} &= qS - \frac{\eta V}{N}[(1-\kappa)I + \kappa A] - mV.\end{aligned} \tag{21}$$

Using the next-generation matrix method [9], the infection sub-system of the system (21), which describes the production of new infections and makes change in the states, reads

$$\begin{aligned}\frac{\mathrm{d}E}{\mathrm{d}t} &= \frac{\beta S}{N}[(1-\kappa)I + \kappa A] + \frac{\eta V}{N}[(1-\kappa)I + \kappa A] - (\omega + m)E,\\ \frac{\mathrm{d}A}{\mathrm{d}t} &= \delta\omega E - \nu A - (\gamma_1 + m)A,\\ \frac{\mathrm{d}I}{\mathrm{d}t} &= (1-\delta)\omega E + \nu A - (\gamma + m + d_i)I.\end{aligned} \tag{22}$$

The transmission matrix (F) and the transition matrix (Σ) associated with the system (22) are given by

$$F = \begin{pmatrix} 0 & \kappa\frac{(\beta m + \eta q)}{q+m} & (1-\kappa)\frac{(\beta m+\eta q)}{q+m} \\ 0 & 0 & 0 \\ 0 & 0 & 0 \end{pmatrix}$$

$$\Sigma = \begin{pmatrix} -(\omega + m) & 0 & 0 \\ \delta\omega & -(\nu + \gamma_1 + m) & 0 \\ (1-\delta)\omega & \nu & -(\gamma + m + d_i) \end{pmatrix}. \tag{23}$$

Then the deterministic basic reproduction number (DBRN) R_{0V}^D of (21) is the spectral radius of the next-generation matrix $-F\Sigma^{-1}$, i.e. $R_{0V}^D = \rho(-F\Sigma^{-1})$, where $\Sigma^{-1} =$

$$\begin{pmatrix} -\frac{1}{\omega+m} & 0 & 0 \\ -\frac{\delta\omega}{(\omega+m)(\nu+\gamma_1+m)} & -\frac{1}{\nu+\gamma_1+m} & 0 \\ -\frac{\delta\omega\nu+(\nu+\gamma_1+m)(1-\delta)\omega}{(\omega+m)(\nu+\gamma_1+m)(\gamma+m+d_i)} & -\frac{\nu}{(\nu+\gamma_1+m)}\times\frac{1}{(\gamma+m+d_i)} & -\frac{1}{\gamma+m+d_i} \end{pmatrix}.$$

Thus, $R_{0V}^D = \frac{\omega(\beta m+\eta q)\{\kappa\delta(\gamma+m+d_i)+(1-\kappa)\delta\nu+(1-\kappa)(1-\delta)(\nu+\gamma_1+m)\}}{(q+m)(\gamma+m+d_i)(\nu+\gamma_1+m)(\omega+m)}$.

If $R_{0V}^D > 1$, then the disease is established in the system.

Appendix 3

Parameter estimation has been done in two steps [20]. First, we fitted the COVID-19 data with the corresponding deterministic system (21) and next the optimal noise intensities are determined to find the best-fitted parameter set for the stochastic system (1). In order to find the best-fitted parameter values of the deterministic system, we used a MATLAB embedded function, lsqcurvefit, which is a nonlinear solver that minimizes the sum of squared difference between the model output and a given data set. Here, a curve $h = g(x, \omega)$, parameterized by $\omega = (\omega_1, \omega_2, ..., \omega_m)$, is fitted with the data points $(x_1, h_1), (x_2, h_2), ...(x_m, h_m)$. The nonlinear

least-squares method finds the certain value of the parameters such that $\Sigma_{i=1}^{m}(g(x_i,\omega)-h_i)^2$ becomes minimum. With this best-fitted parameter set, we then find the optimum noise intensity for the stochastic system (1). Assuming 10,000 random values of σ_1, σ_2, σ_3 and σ_4 between 0 and 1, the stochastic system (2) is simulated 1000 times for each of these four tuples $(\sigma_1,\sigma_2,\sigma_3,\sigma_4)$. We then take the mean of those 1000 evolutions to determine the corresponding r-squared value. The particular value of σ_1, σ_2, σ_3 and σ_4 for which the r-squared value is closest to 1 is our required noise intensity.

Appendix 4

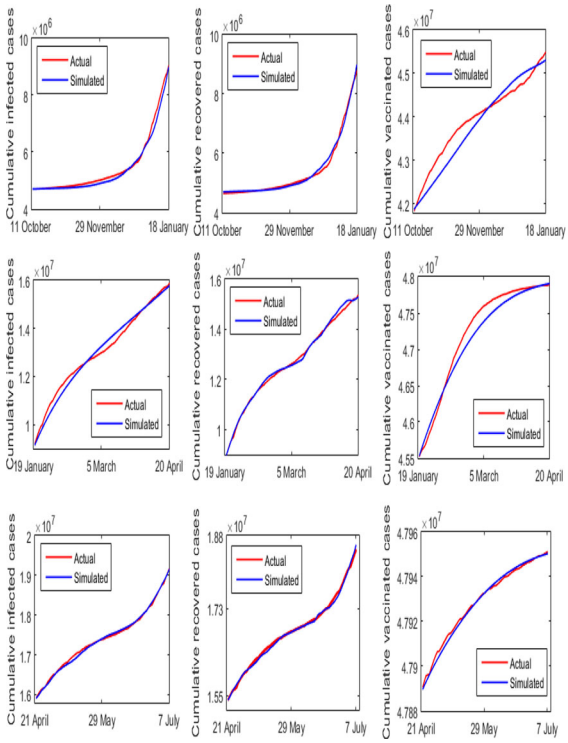

Fig. 7 COVID-19 data fitting with the parameter values and noise intensities as in the Table 2. The first row provides the cumulative actual COVID-19 data (red-coloured curve) of the confirmed, recovered and vaccinated cases in Italy for the period 11 October 2021 to 18 January 2022. The solution (blue-coloured curve) of the stochastic model (1) is the fitted curve with the parameter values of the first row of Table 2. The other rows represent the same with the consecutive periods mentioned in Table 2

References

1. Adak, D., Majumder, A., Bairagi, N.: Mathematical perspective of Covid-19 pandemic: disease extinction criteria in deterministic and stochastic models. Chaos, Solitons Fractals **142**, 110381 (2021)
2. Anastassopoulou, C., Russo, L., Tsakris, A., Siettos, C.: Data-based analysis, modelling and forecasting of the Covid-19 outbreak. PLoS ONE **15**(3), e0230405 (2020)
3. Bhapkar, H., Mahalle, P.N., Dey, N., Santosh, K.: Revisited Covid-19 mortality and recovery rates: are we missing recovery time period? J. Med. Syst. **44**(12), 1–5 (2020)
4. Chen, C., Kang, Y.: The asymptotic behavior of a stochastic vaccination model with backward bifurcation. Appl. Math. Model. **40**(11–12), 6051–6068 (2016)
5. Choudhary, O.P., Choudhary, P., Singh, I.: India's Covid-19 vaccination drive: key challenges and resolutions. Lancet. Infect. Dis. **21**(11), 1483–1484 (2021)
6. Croda, J., Ranzani, O.T.: Booster doses for inactivated Covid-19 vaccines: if, when, and for whom. Lancet Infect. Dis. (2021)
7. in Data, O.W.: The our world in data covid vaccination data. In: ourworldindata.org/covid-vaccinations? country=OWID WRL (2020)
8. Desmet, K., Wacziarg, R.: JUE insight: understanding spatial variation in Covid-19 across the united states. J. Urban Econom. **127**, 103332 (2021)
9. Diekmann, O., Heesterbeek, J., Roberts, M.G.: The construction of next-generation matrices for compartmental epidemic models. J. R. Soc. Interface **7**(47), 873–885 (2010)
10. Dolgin, E., et al.: Covid vaccine immunity is waning-how much does that matter. Nature **597**(7878), 606–607 (2021)
11. Furuse, Y.: Simulation of future covid-19 epidemic by vaccination coverage scenarios in Japan. J. Global Health **11** (2021)
12. Ghostine, R., Gharamti, M., Hassrouny, S., Hoteit, I.: An extended SEIR model with vaccination for forecasting the Covid-19 pandemic in Saudi Arabia using an ensemble Kalman filter. Mathematics **9**, 636 (2021)
13. Han, Q., Chen, L., Jiang, D.: A note on the stationary distribution of stochastic SEIR epidemic model with saturated incidence rate. Sci. Rep. **7**(1), 1–9 (2017)
14. Haque, A., Pranto, T.H., Noman, A.A., Mahmood, A.: Insight about detection, prediction and weather impact of coronavirus (Covid-19) using neural network. ArXiv preprint arXiv:2104.02173 (2021)
15. Juno, J.A., Wheatley, A.K.: Boosting immunity to Covid-19 vaccines. Nat. Med. **27**(11), 1874–1875 (2021)
16. Karako, K., Song, P., Chen, Y., Tang, W.: Analysis of Covid-19 infection spread in Japan based on stochastic transition model. Biosci. Trends **14**, 134–138 (2020)
17. Khajanchi, S., Sarkar, K.: Forecasting the daily and cumulative number of cases for the Covid-19 pandemic in India. Chaos Interdiscip. J. Nonlinear Sci. **30**(7), 071101 (2020)
18. Kurmi, S., Chouhan, U.: A multicompartment mathematical model to study the dynamic behaviour of Covid-19 using vaccination as control parameter. Nonlinear Dyn. **109**, 1–17 (2022)

19. Majumder, A., Adak, D., Bairagi, N.: Persistence and extinction criteria of Covid-19 pandemic: India as a case study. Stoch. Anal. Appl. 1–125 (2021)
20. Majumder, A., Adak, D., Bairagi, N.: Persistence and extinction of species in a disease-induced ecological system under environmental stochasticity. Phys. Rev. E **103**(3), 032412 (2021)
21. Majumder, A., Adak, D., Bairagi, N.: Phytoplankton-zooplankton interaction under environmental stochasticity: survival, extinction and stability. Appl. Math. Model. **89**, 1382–1404 (2021)
22. Manski, C.F., Molinari, F.: Estimating the Covid-19 infection rate: anatomy of an inference problem. J. Econom. **220**(1), 181–192 (2021)
23. Mao, X.: Stochastic Differential Equations and Applications. Elsevier, Amsterdam (2007)
24. Merow, C., Urban, M.C.: Seasonality and uncertainty in global Covid-19 growth rates. Proc. Natl. Acad. Sci. **117**(44), 27456–27464 (2020)
25. Mondal, C., Adak, D., Majumder, A., Bairagi, N.: Mitigating the transmission of infection and death due to SARS-COV-2 through non-pharmaceutical interventions and repurposing drugs. ISA Trans. (2020)
26. Moore, S., Hill, E.M., Tildesley, M.J., Dyson, L., Keeling, M.J.: Vaccination and non-pharmaceutical interventions for Covid-19: a mathematical modelling study. Lancet. Infect. Dis. **21**(6), 793–802 (2021)
27. Musa, M.R., Iyaniwura, S.: Assessing the potential impact of immunity waning on the dynamics of Covid-19: an endemic model of Covid-19. MedRxiv (2021)
28. Paul, A., Chatterjee, S., Bairagi, N.: Covid-19 transmission dynamics during the unlock phase and significance of testing. medRxiv (2020)
29. Paul, A., Chatterjee, S., Bairagi, N.: Prediction on Covid-19 epidemic for different countries: focusing on South Asia under various precautionary measures. Medrxiv (2020)
30. Perc, M., Gorišek Miksić, N., Slavinec, M., Stožer, A.: Forecasting Covid-19. Front. Phys. **8**, 127 (2020)
31. Petrov, V.V.: On the strong law of large numbers. Theor. Probab. Appl. **14**(2), 183–192 (1969)
32. Prem, K., Liu, Y., Russell, T.W., Kucharski, A.J., Eggo, R.M., Davies, N., Flasche, S., Clifford, S., Pearson, C.A., Munday, J.D., et al.: The effect of control strategies to reduce social mixing on outcomes of the Covid-19 epidemic in Wuhan, China: a modelling study. Lancet Public Health **5**(5), e261–e270 (2020)
33. Pritchard, E., Matthews, P.C., Stoesser, N., Eyre, D.W., Gethings, O., Vihta, K.D., Jones, J., House, T., VanSteen-House, H., Bell, I., et al.: Impact of vaccination on new SARS-COV-2 infections in the united kingdom. Nat. Med. **27**, 1–9 (2021)
34. Rabiu, M., Iyaniwura, S.A.: Assessing the potential impact of immunity waning on the dynamics of cCovid-19 in South Africa: an endemic model of Covid-19. Nonlinear Dyn. **109**, 1–21 (2022)
35. Roghani, A.: The influence of Covid-19 vaccine on daily cases, hospitalization, and death rate in tennessee: a case study in the United States. JMIRx Med **2**(3), e29324 (2021)
36. Rossman, H., Shilo, S., Meir, T., Gorfine, M., Shalit, U., Segal, E.: Covid-19 dynamics after a national immunization program in Israel. Nat. Med. **27**, 1–7 (2021)
37. Sanyaolu, A., Okorie, C., Marinkovic, A., Patidar, R., Younis, K., Desai, P., Hosein, Z., Padda, I., Mangat, J., Altaf, M.: Comorbidity and its impact on patients with Covid-19. SN Compr. Clin. Med. 1–8 (2020)
38. Sarkar, K., Khajanchi, S., Nieto, J.J.: Modeling and forecasting the Covid-19 pandemic in India. Chaos, Solitons Fractals **139**, 110049 (2020)
39. De la Sen, M., Ibeas, A.: On an SE(Is)(Ih)AR epidemic model with combined vaccination and antiviral controls for Covid-19 pandemic. Adv. Differ. Equ. **2021**(1), 1–30 (2021)
40. de Sousa, L.E., de Oliveira Neto, P.H., da Silva Filho, D.A.: Kinetic Monte Carlo model for the Covid-19 epidemic: impact of mobility restriction on a Covid-19 outbreak. Phys. Rev. E **102**(3), 032133 (2020)
41. WHO: Covid-19 public health emergency of international concern (PHEIC). In: Global Research and Innovation Forum (2020)
42. WHO: who-prequalification of medical products (ivds, medicines, vaccines and immunization devices, vector control). In: COVID-19 vaccines WHO EUL issued, pp. https://extranet.who.int/pqweb/vaccines/vaccinescovid--19--vaccine--eul--issued. WHO (2021)
43. Yang, Q., Mao, X.: Stochastic dynamical behavior of sirs epidemic models with random perturbation. Math. Biosci. Eng. **11**(4), 1003–1025 (2014)
44. Zhai, S., Luo, G., Huang, T., Wang, X., Tao, J., Zhou, P.: Vaccination control of an epidemic model with time delay and its application to Covid-19. Nonlinear Dyn. **106**(2), 1279–1292 (2021)
45. Zhang, Y., You, C., Cai, Z., Sun, J., Hu, W., Zhou, X.H.: Prediction of the Covid-19 outbreak based on a realistic stochastic model. MedRxiv (2020)
46. Zhou, D., Liu, M., Liu, Z.: Persistence and extinction of a stochastic predator-prey model with modified Leslie–Gower and Holling-type II schemes. Adv. Differ. Equ. **2020**(1), 1–15 (2020)
47. Zhou, Y., Zhang, W., Yuan, S.: Survival and stationary distribution of a sir epidemic model with stochastic perturbations. Appl. Math. Comput. **244**, 118–131 (2014)